

Aerospace Engineering Department
Auburn University
Auburn, Alabama

14-05-91
73702
P. 70

THE FM-007, AN ADVANCED JET COMMUTER FOR HUB TO SPOKE TRANSPORTATION

Presented to : Dr. J. Nichols

Presented by: Peter Blouke
George Engel
Suzanne Fordham
Steve Layne
Joel Moore
Fred Shaver
Doug Thornton

Date Presented: 14 May, 1991

(NASA-CR-189988) THE FM-007: AN ADVANCED
JET COMMUTER FOR HUB TO SPOKE TRANSPORTATION
(Auburn Univ.) 70 p CSCL 01C

N92-20267

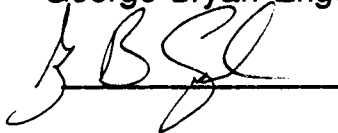
Unclas
63/05 0073902

SIGNATURE PAGE

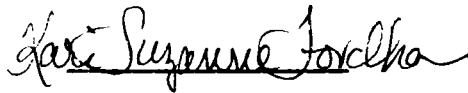
Peter Scott Blouke



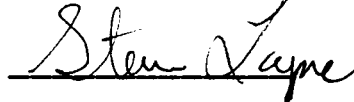
George Bryan Engel



Kari Suzanne Fordham



Steven James Layne



Joel David Moore



Frederick Martin Shaver



Douglas Hershal Thornton Jr.



ABSTRACT

Due to the increasing need for new commuter aircraft, we propose the FM-007, a technologically advanced jet-propelled short-takeoff and landing (STOL) airplane. The proposed commuter is designed for hub to spoke air travel. In order to reduce drag, natural laminar flow technology is integrated into the design using the natural laminar flow airfoil section, HSNLF (1) 0213F, for the wing. A three lifting surface configuration provides for more efficient cruise flight. This unique design includes a small forward wing (canard), a rear-mounted high aspect ratio main wing, and a small horizontal stabilizer high atop the vertical tail. These three surfaces act together to reduce drag by minimizing the downward force the horizontal stabilizer has to account for due to the nose-down pitching moment.

Commuter aircraft must also incorporate passenger comfort. This is achieved by providing a spacious pressurized cabin with a large galley and reduced cabin noise due to incorporation of noise reduction gear. A basic oval design is adopted, as opposed to a circular design in order to allow for the seating of five passengers abreast. Instead of using standard aluminum alloys, an aluminum-lithium alloy is used for its low density.

To achieve STOL capability, an over the wing blown flap is employed using a Rolls Royce Tay series engine. In order to insure that STOL capability is maintained during an engine failure the engines are cross coupled, allowing the operating engine to take over for the out engine.

TABLE OF CONTENTS

<u>Section</u>	<u>Page</u>
Signature Page	ii
Abstract	iii
List of Symbols	v
List of Figures	viii
List of Tables	x
Introduction	1
Cabin Design	2
Initial Configuration	5
Structures	9
Aerodynamics	20
Performance	27
Avionics	30
Summary and Conclusions	32
References	55
Appendix A	57

LIST OF SYMBOLS

<u>Symbol</u>	<u>Description</u>	<u>Units</u>
$a=C_{L\alpha}$	Airplane lift-curve slope	/deg
a_o	Sectional Lift Curve Slope	/deg
AR	Aspect Ratio	-
a_{wb}	Wing-Body Configuration	
	Lift Curve Slope	/deg
b	Wing Span	f t
b_f	Maximum Width of Fuselage	f t
b_{ref}	Reference Span	f t
b_s	Structural Span	f t
c	Mean Aerodynamic Chord	f t
C_D	Coefficient of Drag	-
C_L	Coefficient of Lift	-
C_{Lmax}	Maximum Lift Coefficient	-
CG	Center of Gravity	f t
C_J	Moment Coefficient of Thrust	-
$C_{m\alpha}$	Slope of Pitching Moment	
	vs. Angle of Attack	-
c_r	Root Chord	f t
c_t	Tip Chord	f t
D	Drag	lbs
D_t	Distance Between Quarter Chord Point	
	of Wing and Horizontal Tail Root.	f t
e	Oswald's Efficiency Factor	-
FF	Fuel Flow Rate	lbm/s
g	Gravitational Constant	ft/sec ²
h	CG Position, Fraction of Mean Chord	-
h_n	Neutral Point of Airplane, Fraction of c	-
h_{nw}	Neutral Point of Wing, Fraction of c	-
h_{nwb}	Neutral Point of Wing-Body Combination	-

LIST OF SYMBOLS

<u>Symbol</u>	<u>Description</u>	<u>Units</u>
h_t	Maximum Height of Fuselage	f t
K	Interference Correction Factors	-
L	Airplane Total Lift	lbs
L_c	Lift of Canards	lbs
L_t	Lift of Horizontal Tail	lbs
L_w	Lift of Wing	lbs
l_t	Distance Between CG and Tail	
	Aerodynamic Center	f t
n_{ult}	Ultimate Load Factor	-
S	Planform Area of Wing	sq.ft
S_c	Planform Area of Canard	sq.ft
S_G	Gross Shell Area of Fuselage	sq.ft
SPFC	Specific Fuel Consumption	$\frac{\text{lb.fu}}{\text{hr.lb(T)}}$
S_{REF}	Reference Area	sq.ft
S_t	Planform Area of Tail	sq.ft
S_w	Planform Area of Wing with no Flap	sq.ft
S_{wet}	Wetted Area	sq.ft
T	Thrust	lbs
T_{av}	Thrust Available	lbs
T_{req}	Thrust Required	lbs
T_{to}	Thrust at Takeoff	lbs
t_r	Maximum Thickness of the Root Chord	f t
V	True Airspeed	ft/sec
V_{CR}	Cruise Velocity	ft/sec
V_D	Design Dive Speed	ft/sec
V_{Ht}	Horizontal Tail Volume, $S_t l_t / S_c$	-
V_{Hc}	Canard Volume, $S_c l_c / S_c$	-
V_s	Stall Velocity	ft/sec
W	Airplane Weight	lbs

LIST OF SYMBOLS

<u>Symbol</u>	<u>Description</u>	<u>Units</u>
W_C	Weight of Canards	lbs
W_f	Weight of Fuselage	lbs
W_G	Gross Weight	lbs
W_g	Maximum Zero Fuel Weight	lbs
W_H	Weight of Horizontal Tail	lbs
W_{nc}	Weight of Nacelles	lbs
W_{sc}	Weight of Control Surfaces	lbs
W_{to}	Weight at Takeoff	lbs
W_{uc}	Weight of Undercarriage	lbs
W_V	Weight of Vertical Tail	lbs
W_w	Weight of Wing	lbs
w	Wing Loading, W/S	lb/ft ²
x	Aerodynamic Center Location from Wing Apex	ft
α	Angle of Attack	deg
α_a	Absolute Angle of Attack	deg
ϵ	Downwash Angle	deg
λ	Taper Ratio	-
ρ	Air Density at Cruise	slug/ft ³
ρ_{sl}	Air Density at Sea Level	slug/ft ³
Λ	Sweep Angle	deg

LIST OF FIGURES

<u>Figure</u>	<u>Page</u>
1. FM-007 Front View	36
2. FM-007 Top View	37
3. FM-007 Side View	38
4. Cross-Section of Fuselage	39
5. Top View of Cabin Layout	40
6. Dual Twin Wheel Pattern	41
7. Airfoil Cross-Section of a) main wing, b) canard c) tail.	42
8. CG Location with Lifting Force Locations	43
9. Body-on-Wing and Wing-on-Body Interference Constants.	44
10. C_M versus Alpha	45
11. a) C_D Versus α b) Drag Polar Cruise	46 47
12. a) C_D Versus α (Flap=15) b) Drag Polar at Takeoff (Flap=15)	48 49

LIST OF FIGURES

<u>Figure</u>	<u>Page</u>
13. a) C_D Versus α (Flap=40)	50
b) Drag Polar at Landing (Flap=40)	51
14. Upper Surface Blown Flap	52
15. C_L Versus Alpha for Changes in Flap Deflection and CEO	53
16. AEO Minimum Unstick Airspeeds for Five T/W for the QSRA	54

LIST OF TABLES

<u>Table</u>	<u>Page</u>
1. Cabin Dimensions	4
2. Input Parameters for Initial Configuration Program	5
3. Summary of Initial Configuration Specs	8
4. Component Weights and Areas	15
5. Center of Gravity of Empty A/C	16
6. Center of Gravity of Fully Loaded A/C	17
7. Maximum Forward Limit of C.G.	18
8. Maximum Aft Limit of C.G.	19
9. Mean Aerodynamic Chord for Lifting Surfaces	22
10. Contribution of Lift by Each Surface	23
11. C_{La} and $\partial \epsilon / \partial \alpha$ for Each Component	24
12. Drag at Various Conditions	26
13. Lift Coefficients	27
14. Navigation and Communication Equipment	30
15. FM-007 Aircraft Specifications	34

INTRODUCTION

The need for more advanced commuter aircraft is now emerging due to the aging of current aircraft such as the DC-9 and the Boeing-737. Also the need for hub to spoke service is increasing because of the rapid growth of airports which are already congested. To alleviate this problem advanced technology must be applied to new commuter aircraft to shorten runway lengths, increase payload, and decrease fuel consumption.

The specifications for the FM-007, an advanced design in jet propelled commuters, include a maximum range of 500 nautical miles and a cruise speed of Mach 0.7. In order to reduce drag, the plane has natural laminar flow surfaces over much of the wing and body. To satisfy the demand for increased passenger capacity the plane is designed for a maximum capacity of 70 economy seats or can be modified to incorporate first class and economy seats depending on the desire of the purchaser.

The FM-007 has been designed utilizing the three-lifting surface configuration (Figures 1,2,3). The wings were located far back in order to obtain a better center of gravity location. From this, the size and placement of the three lifting surfaces along with the static margin were determined. Then the avionics layout for the cockpit was arranged. State of the art cathode ray tube (CRT) avionics from Bendix/ King and Honeywell will be implemented into the cockpit design. Landing gear structure for the FM-007 incorporates a dual twin wheel configuration, tricycle style. Experimental aluminum alloys such as aluminum lithium will be used in place of standard aluminum alloys to lighten the structure. Aluminum lithium alloys with high strength characteristics will be the only lithium based alloys considered for the structural design.

In order to meet the above specifications, the FM-007 incorporates an upper surface blown flap using a Coanda flap and a TAY 620 modular engine.

CABIN DESIGN

In designing the cabin of the FM-007 special attention was given to passenger comfort. A fuselage of length 92.67 feet with a cross sectional cabin dimension of 10.5 feet wide and 9 feet high was created with five passengers abreast (Figure 4). Three seats were placed on the right and two on the left with each seat having a 17 inch width and a height of 42 inches. On the right side a space of three inches was allowed for the width of the armrest and two inches on the left side. More room was allowed between seats on the right side in order to give passengers extra room. The aisle width is 19 inches and the height is 6 feet 10 inches. An approximate volume of 3.1 cubic feet per passenger is allotted for carry on baggage and 400.0 cubic feet for the luggage compartment at the rear of the fuselage. The undercarriage stowage is allotted for controls, airstair and landing gear. These dimensions were developed in accordance with the standards for commuter aircraft design¹.

Two spaces for wardrobe were designed with a total approximate floor area of 9.56 square feet. These are located to best accommodate the passengers, one in front and one in back of the cabin (Figure 5). The two restrooms, which are located rearward are given approximate floor areas of 14.5 square feet each. The large galley which is located in the front of the cabin has an approximate floor area of 14.44 square feet. In order to best accommodate the flight attendants, seats with a 15 inch width were allocated by the galley.

In accordance with FAR 25.807 the FM-007 was designed with Type I and Type III emergency exits. These exits are located forward and rearward in the cabin. The rearward Type III exit leads onto the wing, thus allowing easier exiting during emergencies. Passengers enter the plane through the Type I, 3 foot by 6 foot doors, placed on either side in the front of the cabin.

The cockpit of the plane is 5.5 feet in length, allowing considerable space for the pilot, co-pilot, a jump seat and flight systems. The nose of the plane is suitable for housing radar equipment, etc. By using Torenbeek¹, page 78-79, the volume of the luggage was estimated to be 196 cubic feet. The FM-007 has ample room in it's cargo compartment with an approximate volume of 400 cubic feet. Table 1 gives the dimensions for the cabin design.

Table 1. Cabin Dimensions

Fuselage length	92.67 feet
Cross sectional fuselage width	10.5 feet
Cross sectional fuselage height	9.0 feet
Number of passengers	70
Seat width	17 inches
Seat pitch	36 inches
Seat height	42 inches
Arm rest right side (three seats)	3 inches
Arm rest left side (two seats)	2 inches
Seats abreast	5
Aisle width	19 inches
Aisle height	82 inches
Carry on baggage allotment	3.1 cu.feet/person
Wardrobe (total floor area)	9.56 sq feet
Restroom	14.5 sq. feet/each
Galley	14.44 sq. feet
Flight attendant seat width	15 inches
Door	3X6 foot
Cockpit length	5.5 feet
Carry on baggage volume	217 cu. feet
Luggage compartment hold	400 cu. feet

INITIAL CONFIGURATION

In order to determine initial estimates of the payload, empty, fuel, and gross weight, the wing area and span, and thrust required, a Fortran 77 program, Program 1, was written. The input parameters listed in Table 2 are initial estimates and calculations based on other comparable aircraft. Program 1 performs iterations on airload equations given these input parameters.

Table 2 . Input Parameters for Initial
Configuration Program

Stall Velocity (VS)	164.45 ft/sec
Maximum Lift Coefficient (CLMAX)	1.8
Aspect Ratio (AR)	7.5
Parasite Drag Coefficient (CDO)	0.016
Cruise Velocity (V _{CR})	462 knots
Oswald's Efficiency Factor (e)	0.83
Air Density at 30,000 feet (ρ)	0.0008907
Range (R)	575.76 miles
Thrust Available (TAV) at 30,000 ft	5600.0 pounds
Thrust Available at Sea Level (TAVSL)	20000.0 pounds
Fuel Flow Rate (FF)	1932.0 pounds / hr

The first step of the program was to calculate the gross weight of the aircraft. It was determined by:¹

$$\begin{aligned} \text{Payload Weight} &= 200\text{lb} \cdot \# \text{ of Passengers} & (1) \\ W_G &= \text{payload weight} / (0.3) & (2) \\ \text{Fuel Weight} &= 0.15 \cdot W_G & (3) \end{aligned}$$

Once the gross weight was determined, the wing area was calculated from the load factor, W/S, which was calculated by

taking the average of the middle and lower lines from Figure 7.33 of Ref. 2:

$$x = \sqrt[3]{W_G} \quad (4)$$

$$\text{Middle Line} = 2.24(x-6) \quad (5)$$

$$\text{Lower Line} = 1.54(x-6) \quad (6)$$

$$S = \frac{W_G}{\frac{\text{Mid. Line} + \text{Low. Line}}{(2.24 + 1.54)/2.0}} \quad (7)$$

$$b = \sqrt{AR S} \quad (8)$$

From these calculated values, the drag or thrust required was calculated using:

$$x = \frac{1}{2} C_{D0} \rho (V_{CR})^2 S \quad (9)$$

$$y = \frac{2.0}{\pi \rho e} \left(\frac{W_G}{b V_{CR}} \right)^2 \quad (10)$$

$$\text{Drag} = \text{Thrust Required} = x + y \quad (11)$$

After the thrust required was calculated, the fuel weight was determined using the thrust available at sea level, range, and the following calculations:

$$x = \frac{\text{Thrust Required}}{\text{Thrust Available}} \quad (12)$$

$$\text{Thrust Rated} = x \cdot T_{av} \text{ at Sea Level} \quad (13)$$

$$SPFC = \frac{FF}{T_{av}} \quad (14)$$

$$FF1 = SPFC * T_{req} \quad (15)$$

$$Endurance = \frac{Range}{0.6818 V_{CR}} \quad (16)$$

$$Fuel\ Weight = Endurance (FF1) \quad (17)$$

After these values were computed, a new gross weight estimate was calculated using:

$$W_G = \frac{Payload\ Weight + Fuel\ Weight}{1 - 0.55} \quad (18)$$

Then the program iterates ten times. The gross weight, wing area, wing span, and thrust required, become constant values after ten iterations. The values listed in Table 3 are initial computations and may change during the design process.

Table 3. Summary of Initial Configuration Specifications

Component	Specification
Payload Weight	10140 pounds
Empty Weight	14735 pounds
Fuel Weight	1915 pounds
Gross Weight	26791 pounds
Wing Area	533.3 sq. feet
Wing Span	63.2 feet
Aspect Ratio	10
Total Thrust Required at 30,000 ft	3500 pounds
Number of Engines	2
Thrust Available at 30,000 ft	2800 pounds / engine
Thrust Available at Sea Level	13,850 pounds / engine
Fuel Flow	1932 pounds /hr

STRUCTURES

Materials

Materials are an integral part of the FM-007. Instead of using standard aluminum alloys, aluminum alloys containing lithium have been chosen for most of the airplane. The fuselage will be composed primarily of Al2090, an aluminum-copper-lithium-magnesium alloy. This alloy is comparable to the standard Al2024 aluminum-copper alloys used in airplanes today but has a lower density. The density of a standard aluminum alloy is approximately 3.5 g/cm^3 (Ref. 3) while the aluminum-lithium alloy, Al2090, has a density of 2.59 g/cm^3 (Ref. 4).

Also, when considering compound structures, the wings have been given special attention, since the wings of an airplane are usually constructed of more than one material. The wing is primarily constructed of aluminum alloys; on the lower surface of the wing, the Al2090 alloy will be used because of the cyclic tension loading. Al2090 has a tensile strength of 77 ksi in the longitudinal direction and 73 ksi in the transverse direction⁴. This fact proves that Al2090 can withstand high tensile loading and will fit the lower wing skin criteria. The aluminum lithium alloy, Al8085, has similar (or superior) strength characteristics to the standard aluminum zinc alloy, Al7075, but is also about ten percent lighter; therefore, Al8085 will be used for most of the upper wing surface.⁵ There is no need to be concerned about the high temperatures on the upper surface of the wing due to the blown down flap configuration because the exhaust temperatures of the engines are well within the tolerance range of the alloy AL8085. One important point about these aluminum lithium alloys is that they are experimental at this time, and the life span of these materials is unknown.

The internal structure of the wings will also be made of Aluminum Lithium alloys. Al2090 will be the main alloy used in the spars. Al2090 is currently used in extruded leading-edge stiffeners

in the wings of the Airbus A330 and A304 which are currently in production⁶. The successful use of Al2090 in these planes proves that Al2090 can be used in the main spar and stiffener structure of the aircraft.

Landing Gear Structure

The undercarriage design requires capability of absorbing energy, both vertically and horizontally, so that during taxiing, liftoff and touchdown no other part of the aircraft will touch the ground. Reduction of instabilities is a must, especially during maximum braking effort, crosswind landings and high-speed taxiing. The undercarriage must be adapted to the load carrying capacity of the airfields from which the aircraft is intended to operate.

Even though the dimensions of the undercarriage are small in comparison to the wing and fuselage, it must not be regarded merely as an accessory but as an important part of the structure. The undercarriage's weight consists of about 3% of the maximum takeoff weight and one-half of the structural weight of the wing.

The following considerations have an effect on undercarriage layout:

1. During the phases of takeoff rotation and liftoff and landing flare-out and touch down, only the wheels should be in contact with the ground. There should be adequate clearance between the runway and all other parts of the aircraft, such as the rear fuselage, the wing-tips and the engine pods.
2. The inflation pressure of the tires and the configuration of the landing gear should be chosen with consideration of airfields from which the aircraft is designed to operate.

3. The landing gear should absorb the normal landing impact loads and have good landing characteristics. When taxiing over rough ground, no excessive shocks should be transmitted by the landing gear.
4. Braking should be efficient, with the maximum braking force allowed by the condition of the runway being the limiting factor. During crosswind landings and high-speed taxiing there should be no tendency to instabilities such as canting of the aircraft or groundlooping.
5. Suitable structures elements should be provided in the aircraft to serve as attachment points for the landing gear, and there should be sufficient internal space for retraction.¹

The general conclusion is that the tricycle gear has superseded the tail-wheel type almost completely, mainly for reasons of improved stability on the ground, braking, and steering.

The FM-007 will utilize a twin wheel pattern as shown in Figure 6. The multiple wheel undercarriages result in a gain in safety, a flat tire being of lessened consequence. Steerable main landing gear systems will be employed to improve the turning radius, to avoid excessive side loads and to reduce tire wear from scrubbing.

The method of determining the landing gear characteristics was adapted from Synthesis of Subsonic Airplane Design by Egbert Torenbeek¹.

The tire pressure is determined to be 75 pounds per square inch with a load classification number of approximately 15 and an

equivalent single load of 17000 pounds. The tire size of 34 inches by 9.9 inches was determined from the tire pressure.

The diameter of the cylinder of the telescoping main gear was calculated to be 4.41 inches and the maximum tire deflection was 0.03815 inches.

Clearance allowances between the tire and the adjacent parts of the aircraft are based on the maximum dimensions of the inflated tire, a growth allowance due to service, and the effect of centrifugal forces at high-speed rolling, which increases the diameter. Good average values are a four percent increase in maximum width and ten percent increase in diameter during use. The clearance radially around the tire required in connection with centrifugal forces with a landing speed of 183.3 mph and grown tire width of 10.3 inches is found to be 0.8 inches.

The required shock absorber stroke as calculated to be 1.15 feet. The length of the leg required is about three times the required shock absorber stroke for dual and multi-wheel assemblies plus the tire radius plus any change in radius and is equal to 4.96 feet.

The distance between the tire center lines of twin tires should be at least 1.8 times the maximum grown width of the tire of 10.3 inches so that ST is 18.0 inches.

Weights and Center of Gravity

One important consideration in the determination of the performance of an aircraft is the weight of the individual components of the aircraft. One method for finding individual component weights is found in Torenbeek¹.

The initial component weight that was determined was the dry fuselage weight. One step in finding the dry fuselage weight is calculating the wetted area of the fuselage. Equation 19 is the equation used in that weight determination

$$W_f = k_{wf} \sqrt{V_D \frac{l_t}{b_f + h_t} S_G^{1.2}} \quad (19)$$

where k_{wf} is a constant with the value of 0.021. Both the fuselage area and weight are presented in Table 4.

The next component weight calculated was the weight of the wing, where k_w is a constant with the value of 0.0017.

$$W_W = W_G k_W b_s^{0.75} \left[1 + \sqrt{\frac{b_{ref}}{b_s}} \right] n_{ult}^{0.55} \left(\frac{b_s/t_r}{W_G/S} \right)^{0.3} \quad (20)$$

Most of the values used in Equation 20 are given by the initial configuration program presented earlier in this report. The ultimate load factor is derived from FAR 23 and FAR 25⁷. The value of the wing area and weight are presented in Table 4.

The weights of the canards, the horizontal tail, and the vertical tail are calculated in the same manner. The weight of these components is a function of their planform area, the design dive speed and the sweep angle of the component. Equation 21 shows this function

$$\frac{W_h}{S_h k_h} = f \left(\frac{S_h^{0.2} V_D}{\sqrt{\cos \lambda_v}} \right) \quad (21)$$

where k_h is a constant with a value of 1.0 for all three components. The values of the function can be found in Torenbeek.¹ The weights and areas of these components are in Table 4.

The method of determining the weight of the undercarriage, the nose gear and the main gear, used to perform this task is Equation 22,

$$W_{uc} = k_{uc} \left[A + B W_{to}^{0.75} + C W_{to} + D W_{to}^{1.5} \right] \quad (22)$$

where k_{uc} is a constant with a value of 1.0. The constants A, B, C, and D are different for the two components of the landing gear. The table that the constants are determined is in chapter eight of Torenbeek.¹ These weights are in Table 4.

The individual nacelle weights are 5.5% of the take off thrust. These weights are in Table 4. The weight of the surface controls is calculated by Equation 23

$$W_{sc} = k_{sc} W_{to}^{2/3} \quad (23)$$

where k_{sc} has a value of 0.64.¹ This weight is also in Table 4.

Table 4. Component Weights and Areas

Components	Areas	Weights
Fuselage	2558.98 ft ²	7386.21 lb
Wings	533.3 ft ²	1926.108 lb
Canards	84.39 ft ²	506.353 lb
Horizontal Tail	132.468 ft ²	781.561 lb
Vertical Tail	149.675 ft ²	898.05 lb
Nose Gear	- -	238.178 lb
Main Gear	- -	890.66 lb
Surface Controls	- -	574.975 lb
Nacelles x2	- -	1100 lb
Engines x2	- -	6270 lb
Total Weight		20572.09 lb

The weight of the fuel was previously calculated by a computer program. This weight was then used in another computer program which determined the center of gravity of the fuel located within the wings. The program based its calculations on the root chord, the tip chord, the span of the wing, sweep angle, and the weight of the fuel. The answer given by the computer was converted to inches and then recalibrated from the tip of the nose of the airplane. This was done in order to conform the center of gravity of the fuel to the other data of the airplane in the calculation of overall center of gravity. Another computer program was written that determined the center of gravity of the wing based on thickness ratio, tip chord, root chord, the span of the wing, and sweep angle.

This answer was converted to inches and then recalibrated from the tip of the nose of the airplane in order to conform to other data for determination of overall center of gravity.

Once the weights of the different components have been determined, the center of gravity of the components can be ascertained and from that, the center of gravity of the airplane. A spreadsheet was set up with the individual weights and c.g.s (centers of gravity) of the airplane. A spreadsheet was used for ease of calculation; this way, different cases could be studied, including: empty airplane, full airplane, maximum forward and maximum aft c.g.s. Also, using the spreadsheet helped when parts of the airplane were modified to meet stability criteria. Presented below are various tables for calculations of different c.g. values.

Table 5: Center of Gravity of Empty A/C

Component	Weight(lb)	Moment Arm(in)	Moment(in·lb)
Fuselage	7386.21	501.4717	3703975.2
Horizontal Tail	781.561	1061.4	829548.84
Vertical Tail	898.05	939	843268.95
Front Undercarriage	238.178	120	28581.36
Main Undercarriage	890.659	672	598522.84
Canard (both)	506.3526	193.5	97979.23
Totals	10701.0106		6101876.5
Empty Airplane Moment Arm =			570.2143 in
			47.51798 ft

By dividing the total of the moments by the total of the weight (from Table 5), the center of gravity of the empty airplane was found to be 47.5179 feet from the tip of the nose.

Table 6: Center of Gravity of the Fully Loaded A/C

Component	Weight(lb)	Moment Arm(in)	Moment(in•lb)
Empty A/C	10701.0106	570.215	6101876.75
Wings (both)	1926.108	749.185	1443011.22
Engines (both)	6270	670.96	4206919.2
Nacelles (both)	1100	670.96	738056.0
Crew	360	102.8125	37012.5
Passengers	12260	620.1663	7603238.88
Baggage	2450	854.76	2094162.0
Fuel	1915.9609	712.44	1365007.18
Totals	36983.0795		23589283.7
Fully Loaded Airplane c.g. Moment Arm=			637.8398 in
			53.153324ft

The total of the moments was divided by the total of the weight (from Table 6) and the center of gravity of the fully loaded airplane was found to be 53.1533 feet.

Table 7. Maximum Forward Limit of Center of Gravity

Component	Weight(lb)	Moment Arm(in)	Moment(in•lb)
Empty A/C	10701.0	-67.6249	-723654.77
Engines (both)	6270	33.1201	207663.027
Nacelles(both)	1100	33.1201	36432.11
Wings (both)	1926.108	111.3451	214462.687
Crew	360	-535.0274	-192609.86
Passengers	12260	-17.6736	-216678.33
Baggage	0	216.9201	0
Fuel	1915.9609	74.6001	142930.874
	36539.370		-531454.27
Maximum forward c.g. Moment Arm=		-14.5447in	-1.21205ft

When finding the maximum forward c.g., only the empty airplane, the engines, nacelles, and wings, crew, passengers and baggage, fuel, and crew were considered. The total of the moments about the fully loaded c.g. was divided by the total of the weight (from Table 7) so that the center of gravity was found to be 1.2121 feet ahead of the fully loaded c.g. The moment arm measurement was changed in order to be able to better picture the movement of the c.g. about its fully loaded location.

Table 8. Aft Limit of Center of Gravity

Component	Weight(lb)	Moment Arm(in)	Moment(in·lb)
Empty A/C	10701.0106	-67.6249	-723654.7
Wings (both)	1926.108	111.3451	214462.687
Engines(both)	6270	33.1201	207663.027
Nacelles (both)	1100	33.1201	36432.11
Crew	360	-535.0274	-192609.86
Baggage	2450	216.9201	531454.245
Fuel	1915.9609	74.6001	142930.874
	36539.3709		216678.308
Maximum aft c.g. Moment Arm=		5.92999 in 0.49416 ft	

When determining the maximum aft movement of the c.g., only the empty airplane, the engines, nacelles, and wings, the crew, and the fuel. When fulfilling these requirements, the total of the moments divided by the total of the weight (from Table 8) equals to the c.g., which was determined to be 0.4942 feet back from the c.g. of the fully loaded airplane (going towards the tip of the tail). From the maximum forward and the maximum aft c.g.s, notice that the c.g. has a maximum movement of 1.7063 feet.

The tables above indicate that the c.g. movement for the airplane will not have a significant effect on the aerodynamics of the airplane and the stability of the airplane depends on the aerodynamicists calculations.

AERODYNAMICS

The emergence of new advanced configuration technology has provided the necessary means of increasing aircraft performance while minimizing the increase in weight and drag. The FM-007 has introduced the three lifting-surface design to the commuter aircraft market.

This unique design includes a small forward wing (canard), a rear-mounted high aspect ratio main wing, and a small horizontal stabilizer high atop the vertical tail. These three surfaces act together to reduce drag by minimizing the downward force the horizontal stabilizer has to account for due to the nose-down pitching moment.

For a conventional two-surface configuration the nose-down pitching moment is counteracted by a force acting downward on the horizontal tail. This negative lift acting on the horizontal stabilizer can account for as much as 20 percent of the aircraft lift⁸. Therefore, the main wing must counteract this force by producing extra lift equal to the downward force plus the weight of the airplane. Thus, the main wing is designed larger than necessary which increases drag.

When a three-lifting surface design is used, the lift created by the canards counteracts the downward pitching moment. Thus, the main wing actually needs to produce less lift than the aircraft's weight since the canard adds to lift so that the sum of all lift produced by the surfaces, during cruise, must only equal the aircraft weight. Because the canards provide nearly all of the balancing forces in cruise, the wing area can be greatly reduced.

More aircraft would probably utilize canards if it were not for two important problems incurred by implementing such devices. First, balancing out the large nose-down pitching moments that are generated when flaps are deployed, and second, achieving favorable pitch control and stall characteristics.

To address these problems, the FM-007 has incorporated a small horizontal stabilizer. Although a small price is paid in weight

and drag for the use of the horizontal stabilizer and canard, the gains in controllability and cruise performance compensate for it.

The rear-mounted wing and T-tail of the FM-007 will result in a pitch-up tendency, especially at high angles of attack. The aft location of the wing causes a relatively large destabilizing moment-in-pitch as the wing stalls. Proper canard design and wing tailoring compensates for the large pitch-up tendency.

The low mounted wings allow for easier maintenance and accessibility to various aircraft systems. The high-mounted T-tail was designed so that the jet wash will not affect the performance of the tail. Also, the ground effect caused by the wing on the horizontal tail will be significantly lessened for a T-tail configuration.

Because of the increased importance of aircraft fuel efficiency, much research into laminar boundary layer control in the past decade has resulted in progress in the areas of parasite, induced and skin friction drag reduction. Supercritical high aspect ratio wings have resulted in drag reductions up to 15%.

Skin friction drag accounts for 30% to 50% of total cruise drag. The new NACA 6-series natural laminar flow (NLF) airfoils, smooth surfaces and controlled pressure gradients will result in large regions of natural laminar flow. As a result skin friction drag can be reduced nearly 90%.

Because the FM-007 is designed for short takeoff and landing capabilities, laminar flow wings were utilized, thus providing lower drag. Although laminar flow technology is relatively new and information about these type airfoils is limited, we chose the HSNLF (1)-0213F airfoil (Figure 7) for the wing. It provides a high coefficient of lift, 0.26 at 2 degrees incidence, and the coefficient of drag is small at Mach 0.7. The tail sections are NACA 0012 airfoils (Figure 7), which were chosen because they provide a C_l of 0.2 at an incident angle of 0.2 degrees. We chose the NACA 2412 (Figure 7) airfoil for the canard which provides a C_l of 0.622 at an angle of incidence equal to 3 degrees. For detailed information on these airfoils see Appendix A.

Stability Analysis

In order to determine the stability characteristics of the FM-007, the basic equations taken from Etkin⁹ and Shevell⁷ were applied. Once the center of gravity for the aircraft was obtained, the static analysis of the moment about the center of gravity was determined knowing the lift that each of the lifting surfaces provides and multiplying it by the distance from the CG. See Figure 8.

The mean aerodynamic chord of the three lifting surfaces can be calculated by:

$$mac = 2/3 [c_r + c_t - (c_r c_t)/(c_r + c_t)] \quad (24)$$

The mac calculated for each lifting surface is listed in Table 9.

Table 9. Mean Aerodynamic Chord for Lifting Surfaces

Component	Mean Aerodynamic Chord
Wing	7.6 feet
Tail	5.8 feet
Canard	3.6 feet

After airfoil selection then the lift and pitching moment is determined. Since C_l is the section lift coefficient, the wing, tail, and canard lift coefficients need to be calculated using the formula:

$$C_L = \frac{(a_0 * \alpha_a)}{[1 + a_0 / (\pi * AR)]} \quad (25)$$

From this the total wing lift can then be calculated by:

$$L_W = \frac{1}{2} C_{LW} \rho V^2 S \quad (26)$$

The tail and canard lift can be calculated using the same formula. Knowing that this lift acts on the quarterchord and the placement of each with respect to the nose, the moment arm of each can then be determined. See Figure 8. The lift of each component calculated and their respective moment arms are given in Table 10.

Table 10. Contribution of Lift by Each Surface*

Component	Lift	Moment Arm
Wing (L_W)	29946.1842 lbs	7.8467 feet
Tail (L_T)	5717.988 lbs	32.9243 feet
Canard (L_C)	11352.061 lbs	37.2253 feet

*contribution by fuselage neglected

The next calculation needed is the $C_{L\alpha}$ for the total aircraft. This is calculated by summing the $C_{L\alpha}$ for each component and referencing it to the wing planform area. $C_{L\alpha}$ for the each lifting surface is calculated by

$$C_{L\alpha \text{ uncorrected}} = a_0 / [1 + (a_0 * 57.3) / (\pi * AR * e)] \text{ per degree} \quad (27)$$

In order to correct for interference effects, body on wing and wing on body, Figure 9. was used and a new value for $C_{L\alpha}$ was calculated by

$$C_{L\alpha \text{ corr.}} = (K_{w(b)} + K_{b(w)}) * (C_{L\alpha \text{ uncorr.}}) \quad (28)$$

The downwash for the wing and canard can be calculated by

$$\varepsilon = C_L / (\pi \cdot AR) \quad (29)$$

Taking the derivative with respect to the angle of attack yields

$$\partial \varepsilon / \partial \alpha = (1 / \pi \cdot AR) / (\partial C_L / \partial \alpha) \quad (30)$$

The values for $C_{L\alpha}$ referenced to the wing planform area and $\partial \varepsilon / \partial \alpha$ are listed in Table 11.

Table 11. $C_{L\alpha}$ and $\partial \varepsilon / \partial \alpha$ For Each Component

Component	$C_{L\alpha \text{corrected}}$ ($\partial C_L / \partial \alpha$)	$\partial \varepsilon / \partial \alpha$
Wing	0.128 per degree	4.0507508×10^{-3}
Canard	0.025 per degree	1.06604×10^{-3}
Tail	0.020 per degree	-----

The horizontal surface volume for the tail and canard was calculated from the following equation,

$$V_H = (l_t c^* S_{t c}) / (c^* S_w). \quad (31)$$

which yields

$$V_{Hc} = 0.77$$

$$V_{Ht} = 1.07$$

Using Etkin⁹, with the sweep angle at 10 degrees, $h_{nwb} = 0.27$.

Therefore, the distance to the neutral point of the wing-body is 2.057 feet. With all of these calculations the neutral point can be determined by

$$h_n - h_{nwb} = V_{Hc} (a_c/a_{wb})[1-(\partial \varepsilon/\partial \alpha)_c] + V_{Ht} (a_t/a_{wb})[1-(\partial \varepsilon/\partial \alpha)_w]^* \quad (32)$$

* as a fraction of the mean aerodynamic chord

Therefore $h_n = 0.497$, so that $h_n c = 3.788 \text{ ft.}$

The static margin is calculated using,

$$h_n - h = 0.94$$

where h was graphically determined to equal 2.85 ft. from Figure 8. Then $C_{m\alpha}$ was calculated by

$$\partial C_m / \partial \alpha = C_{m\alpha} = (h - h_n) a = -0.163 \quad (33)$$

which agrees with the static stability criteria. The C_m versus alpha curve for various elevator deflections has been plotted in Figure 10.

Drag Polars

The drag polars were calculated using the Jan Roskam method of estimating drag polars¹⁰ and theory taken from A Theory of the Jet Flap in Three Dimensions¹¹. Three drag polars were made. One for cruise, one for landing and one for takeoff. The drag polars calculated were:

$$C_D = .0294 + \frac{C_L^2}{26.005} + 1.1566\alpha^3 \quad \text{Cruise} \quad (34)$$

$$C_D = .0441 + \frac{C_L^2}{32.882} + 1.1566\alpha^3 \quad \text{Takeoff} \quad (35)$$

$$C_D = .0861 + \frac{C_L^2}{32.882} + 1.1566\alpha^3 \quad \text{Landing} \quad (36)$$

Figures 11, 12 and 13 show the drag polars and drag coefficient versus alpha for cruise, takeoff and landing. These figures were calculated using a flap deflection of zero for cruise, 15 degrees for takeoff and 40 degrees for landing. They also included a 5% decrease in thrust due to the exhaust scrubbing over the surface of the wing, this is based on NASA QSRA flight test data. These drag polars do not include loss in thrust due to thrust vectoring or to power extraction to run accessories. These were taken into account when determining takeoff and landing distances and total thrust available. Table 12 gives a list of the total drag estimated for normal cruise, takeoff and landing conditions.

Table 12. Drag at Various Conditions

Condition	Velocity (ft/s)	Angle of Attack (deg)	Drag (lbf)
Cruise	740.0	2	4144.0
Takeoff	120.0	10	4042.0
Landing	120.0	10	10,100.0

The drag at cruise is of a comparable amount to that of a similar size aircraft. However during takeoff and landing the drag is far more than a normal aircraft. This is due to the increased induced drag from the blown flaps. The total thrust available from the Tay 620 engines at sea level is 23,500 lbf (this does not include thrust lost due to the spreading of the exhaust over the wing or to its deflection). During cruise the total thrust available is 4800 lbf. With a full load of 40,000 lbs and standard atmospheric conditions the range is 545 nmi. The maximum cruising velocity is Mach 0.85.

PERFORMANCE

Coefficient of Lift During Takeoff and Landing

High lift during takeoff and landing is generated by the use of an upper surface blown flap. An upper surface blown flap works by having the high velocity exhaust from the engine blow over the top of the wing and then vectored downward by deflection of the flap (see Figure 14)¹². The lift can be separated into three components: 1) the basic wing aerodynamic lift, 2) the vector component of the engine thrust in the lift direction, and 3) the wing lift due to super-circulation. The coefficient of lift is determined from theory derived by Makkell and Spence¹¹. This theory gives fairly accurate results up to a 35 degree deflection. From flight data taken from the QRSRA it is shown that for deflections above 40 degrees the lift remains about constant. Therefore for landing conditions the coefficient of lift calculated is for a 35 degree flap deflection and it is assumed that the lift will not increase much above this (see Figure 15).

From Figure 15, a table is made of the takeoff and landing lift coefficients for normal and for one engine out conditions.

Table 13: Lift Coefficients

	Normal	One Engine Out
Takeoff	3.6	3.1
Landing	5.5	4.4

These figures compare well to those determined from flight test of the QRSRA for a wing loading of 75psi¹² (see Figure 15).

Takeoff Performance

The takeoff distance was calculated in accordance with FAR 25 field length requirements.⁷ This requires the takeoff distance to be the greatest of three possible cases: 1) all-engine operating takeoff distance to clear a 35 ft. obstacle plus a 15% distance margin, 2) accelerate and continue the takeoff after a critical engine failure, and 3) decelerate and stop after a critical engine failure. Most of the FAR 25 criteria was adhered to except for the definition of the takeoff climb safety speed as 1.2 times the power off stall airspeed. This is obviously not applicable to a powered lift aircraft. Instead the climb safety speed was taken as 1.2 times the one engine out power on stall velocity. This is determined to be about 120.0 ft/sec.

In order for a powered lift aircraft to be viable it must be able to maintain its STOL performance even with one engine out. The FM-007 does this by cross-coupling the engines such that the turbine of one engine powers the fan of the other. With proper gearing the thrust can be balanced between the engines for a total of 60% of the total thrust. This allows the thrust to be balanced over both wings and thus the lift to be balanced on both wings. Because only a relatively small amount of thrust is needed to maintain a high lift, STOL performance is maintained. Technology for this concept has been developed by General Electric and NASA's Lewis Research center in support of the X-wing, folding tilt rotor and Grumman 698 tilt nacelle concepts¹³. This technology should be directly applicable to the FM-007.

The takeoff run itself is broken up into four separate sections: 1) acceleration from rest to the critical velocity, 2) acceleration from the critical velocity to the rotation velocity, 3) acceleration from the rotation velocity to the lift off velocity, and 4) from the lift off point to the 35 ft obstacle. If at the critical velocity an engine fails then the pilot must apply the brakes and decelerate the plane to a stop. The lift off velocity is given as 1.1 times the minimum all engine on unstick airspeed V_{mu} . V_{mu} is taken from Figure 16¹³ which was made from flight data taken from the QSRA.

From this figure the unstick airspeed is 70 knots or 118 ft/sec. From the stall and unstick velocities the takeoff distance can be calculated. For a lift off velocity of 129.0 ft/sec and a climb safety speed of 144 ft/sec the total takeoff distance is 1500.0 ft. This is the takeoff velocity for a one engine out condition. This is the longest of the three cases and thus the FAR 25 takeoff distance.

This takeoff distance compares to a takeoff distance between 4000-5000 ft for a comparable aircraft. This takeoff distance should allow the FM-007 to takeoff from most airports in the U.S. and possibly even a STOL port such as the one in London, England.

Landing Performance

The landing distance is a little more difficult to calculate. The landing run is divided into a glide distance from a 50 ft height, and a ground roll. The lift coefficient is around 4.5 and the drag coefficient is about 1.0. As stated earlier the lift does not increase greatly after a deflection of about 40 degrees however the thrust available does change with increased deflection. This allows the pilot to control the thrust available with either the throttle or the flaps. The stall velocity can be calculated in a similar manner as above and is calculated to be 110.0 ft/sec. The velocity at the 50 ft obstacle height is 1.3 times the stall velocity and the contact velocity is 1.25 time the stall velocity. Using these numbers the total landing distance is 900.0 ft.

Should an engine fail and the cross coupling not engage the FM-007 can still make a conventional landing. The rudder was not reduced from a conventional size and thus is capable of countering the yaw produced by engine out asymmetric thrust. The landing distance would be well beyond that of a STOL aircraft but still within a conventional airports landing strip.

AVIONICS

The avionics of the FM-007 incorporates the latest in glass cockpit technology with some of the top of the line digital avionics¹⁴.

The basic "T" information such as attitude, altitude, heading, airspeed, and vertical speed along with complete flight direction commands will be contained in the 8X8-inch Primary Flight Display (PFD)(Figure18). The PFD places each of these single instruments into one Cathode Ray Tube (CRT), which reduces weight and also reduces the pilots workload since he does not have to scan several instruments at one time.

Navigation and Communication which are provided by Bendix/King, a subsidiary of the Allied-Signal Aerospace Company, are shown in Table 14.

Table 14. Navigation and Communication Equipment*

System Name	Internal Unit	External Unit	Cost
VHF Transceiver	KTR 908	KF 598A	\$9235
Digital VOR Receiver (NAV)	KNR 634	KFS 564A	\$12300
Digital ADF System	KDF 806	KFS 586A	\$9745
ADF Indicator		KNI 582	\$5110
Digital DME	KDM 706A	KDI 574	\$14180
Transponder	KXP 756	KFS 576	\$7890
Pilot HSI		KPI 553B	\$18440
Copilot HSI		KPI 552B	\$13885
RADAR Altimeter	KRA 405	KNI 415	\$11695
Audio Control Console/Intercom		KMA 24H	\$1585
Digital Weather RADAR System		RDS 86	\$53350
Flight Management System KNS660	KNC 667	KCU 567	\$29435
Total Cost			\$188850

* Bendix/King ¹⁵

Each of the components in Table 14 can be incorporated into the KNS 660 system. The KNS 660 Flight Management System includes the KCU 567 Panel mounted control/display unit and the KNC 667 remote mounted navigation computer/memory/data base. The KNS 660 is an onboard flight management computer that provides the navaid selection and tuning at the touch of a button. It also plans for the ultimate in convenience. This system is designed to interface with either the Electronic Flight Instrument System (EFIS) or standard flight instrument systems.

The FM-007 will incorporate standard instruments for backup such as Altimeter, Airspeed, Attitude, and Vertical Speed indicator. The remaining instruments such as engine instruments will be installed from the manufactures specification. The remaining switches and circuit breakers will be installed as required to meet FAR certification.

SUMMARY AND CONCLUSIONS

The FM-007 is an advanced design commuter aircraft that utilizes the best flight characteristics available. Drag is reduced due to natural laminar flow airfoils, the three lifting surfaces, and a streamlined fuselage design. In order to meet the demand for shorter runway lengths powered lift in the form of an upper surface blown flap is employed to give the aircraft STOL performance. The TAY 620 engines used on the aircraft are some of the most fuel efficient engines available on the market. This helps to decrease the total weight during takeoff due to the decrease in needed fuel. In order to make the FM-007 as light as possible aluminum-lithium alloy 2090-T83 is used extensively. The landing gear is a dual wheel tricycle design which ensures safety in the event of a flat tire and plane stability during takeoff and landing. The avionics of the FM-007 consists of the latest in glass technology and digital instrumentation.

From this information a few conclusions can be drawn about the FM-007. One is that the aircraft does meet the requirements initial set out for it, which were:

- 1) a 500 nautical miles range
- 2) a cruise velocity of Mach .7
- 3) a seating capacity for 70 passengers and their luggage
- 4) the use of laminar flow technology in order to decrease drag
- 5) STOL performance.

The aircraft with a fuel load of 2000 lbs can fly over 545 nautical miles and at a Mach number of .75 if necessary. The STOL performance of the aircraft is such that with a 40,000 lbf load the takeoff distance is under 1,500 ft. This allows the plane to land at most airports in the world and since its runway distance is so short community noise problems are abated.

Another conclusion that can be made from this report is that the FM-007 is not a cheap aircraft. The alluminum-lithium alloy it uses is still fairly new and is only just now beginning to be

introduced into aircraft. It is expected however that its use will increase as it becomes more available and thus its price will drop in the future. Also the price for maintaining a laminar flow aircraft is fairly high. This is due to the fact that laminar flow sections of the aircraft must be kept very clean as compared to a conventional aircraft. And finally the high technology used in the cockpit adds a great deal to the total cost. However again as this technology becomes more common place the price should drop.

A final conclusion that can be made is that the FM-007 should be a fairly safe aircraft. Due to its slow takeoff and landing speeds the pilot has more time to make decisions when an accident occurs. The slow velocities also increase the survivability of the passengers should the plane crash. As more and more planes begin to fill the skies this safety factor could become a very desirable characteristic in modern aircraft.

A summation of the FM-007's specifications is given in Table 15.

Table 15. FM-007 Aircraft Specifications

External Geometry		
Planform Area	533.3	ft ²
Wing Span	73.2	f t
Root Chord	10.0	f t
Tip Chord	4.6	f t
Sweep	10	degrees
M.A.C.	7.28	f t
Thickness Ratio	.134	-
V Tail Area	299.4	ft ²
H Tail Area	264.9	ft ²
Canard Area	84.39	ft ²
Fuselage Length	92	f t
Cross Section Area	74.2	f t
Fuselage Diameter	10.5 by 9.0	f t
Flap Area	191.4	ft ²
Cabin Geometry		
Number of Seats	70	-
Seat Width	17	in
Seat Height	42	in
Seat Pitch	36	in
Arm Rest Right Side	3	in
Arm Rest Left Side	2	in
Seats Abreast	5	-
Aisle Width	19	in
Aisle Height	82	in
Carry on Baggage Allotment	3.1	ft ³ per passenger
Wardrobe (total floor area)	9.56	ft ²
Restroom	14.5	ft ² each
galley	14.44	ft ²

Flight Attendant Seat Width	15	in
Door	3x6	ft
Cockpit Length	5.5	ft
Luggage Volume	196	ft ³
Compartment Hold	400	ft ³
Weights and Center of Gravity		
Empty Weight	20572	lbs
Fuel Weight	2000	lbs
Max Takeoff Weight	40000	lbs
Max Landing Weight	40000	lbs
Forward C.G.	52	ft
Aft C.G.	54	ft
Static Margin	0.9417	ft
Performance		
FAR Takeoff Dist.	1486	ft
FAR Land. Dist	884	ft
Cruise Velocity	Mach .7	-
Stall Speed	120	ft/s
Takeoff Thrust	22000	lb
Wing Loading	75	lb/ft ²
Range	545	nmi

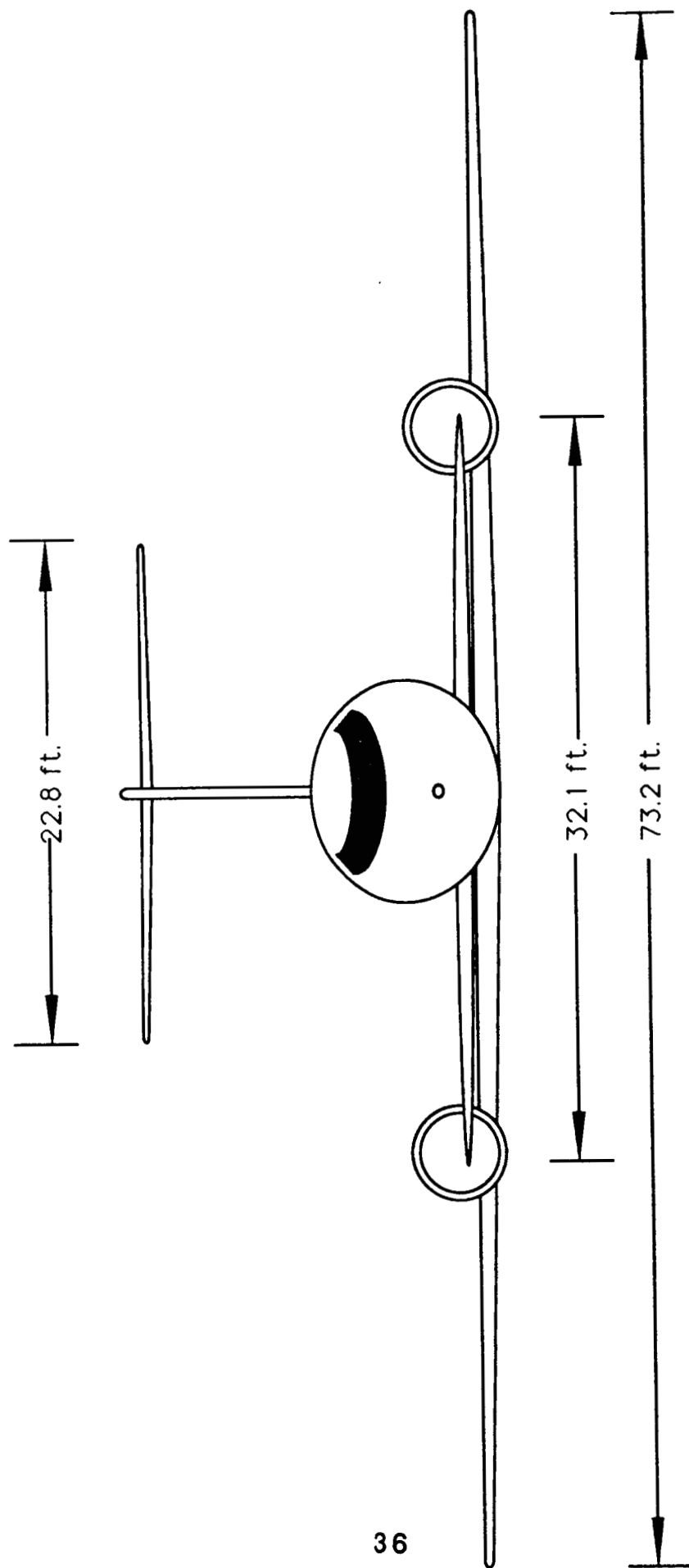


Figure 1: Front View of FM-007

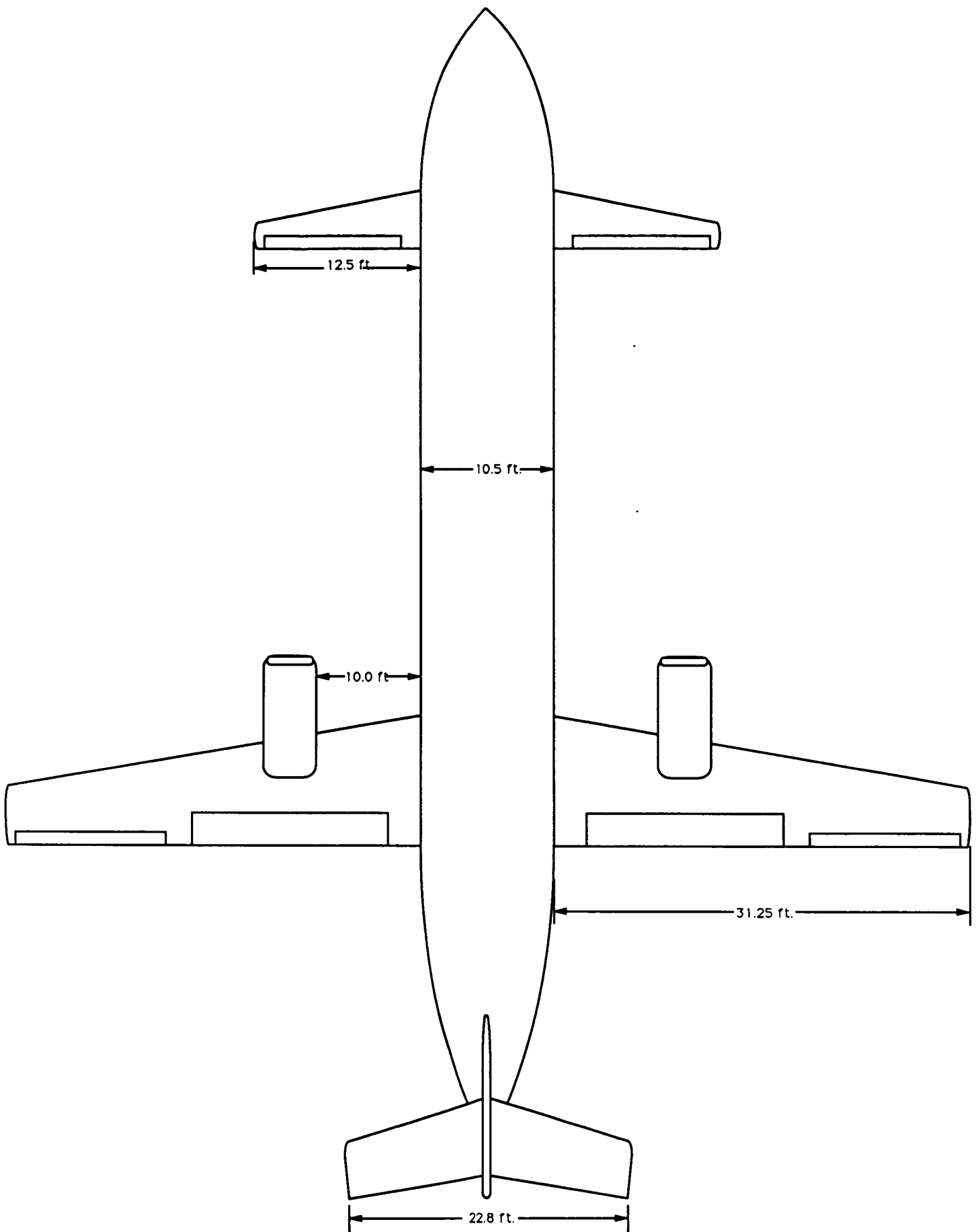
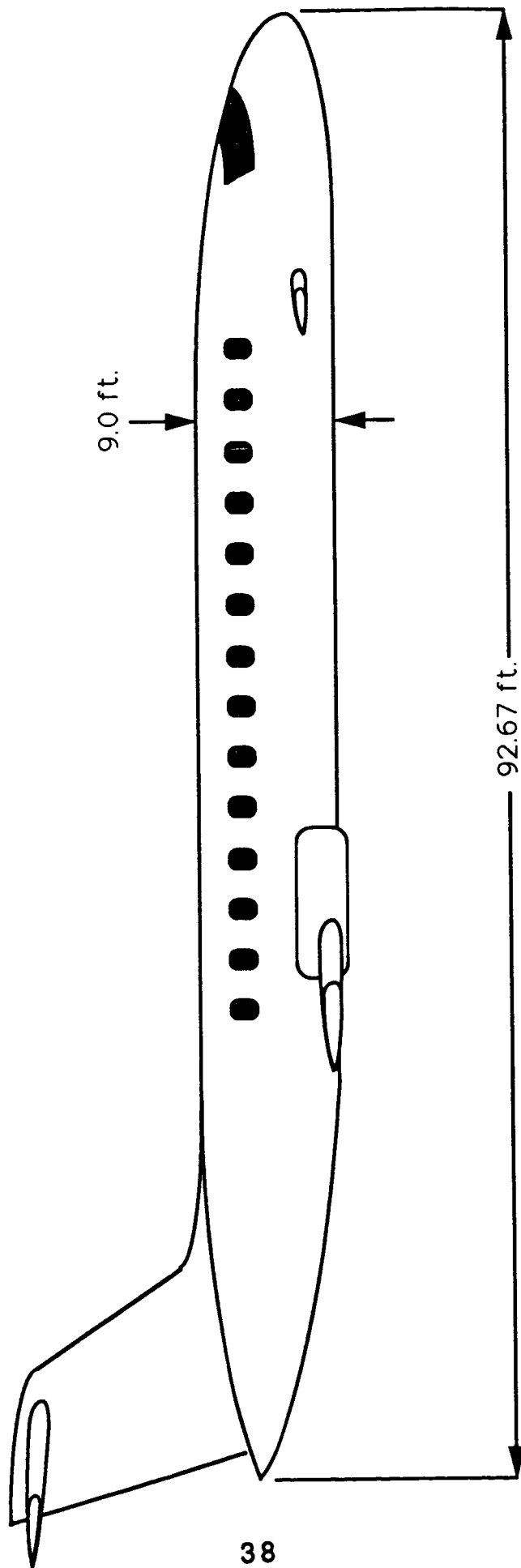


Figure 2: Top View of FM-007



38

Figure 3: Side View of FM-007

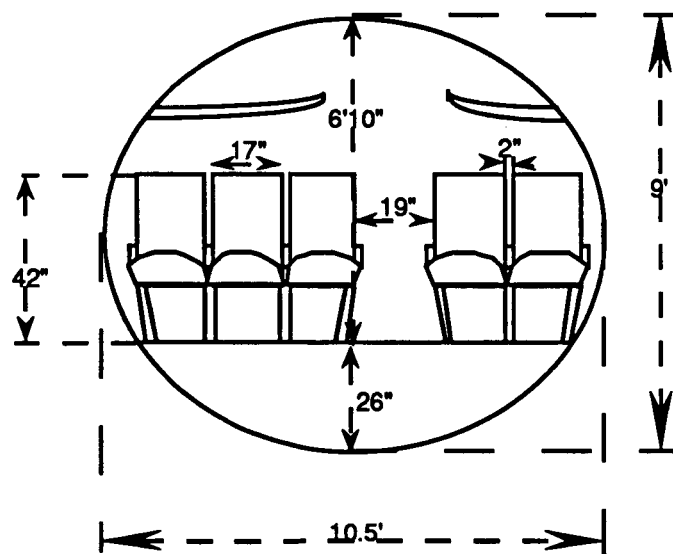


Figure 4. Cross-Section of Fuselage

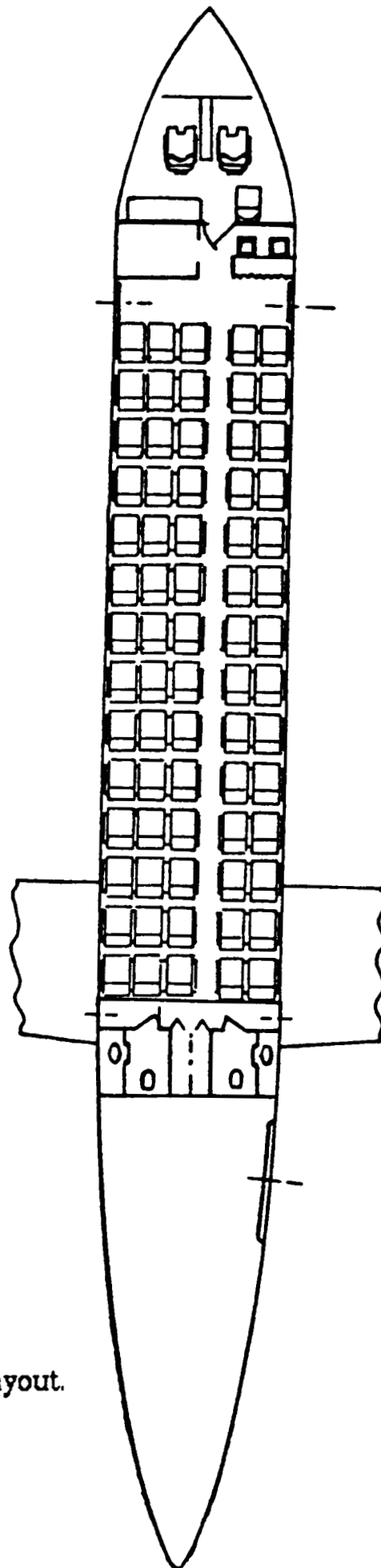


Figure 5 : Top View of Cabin Layout.

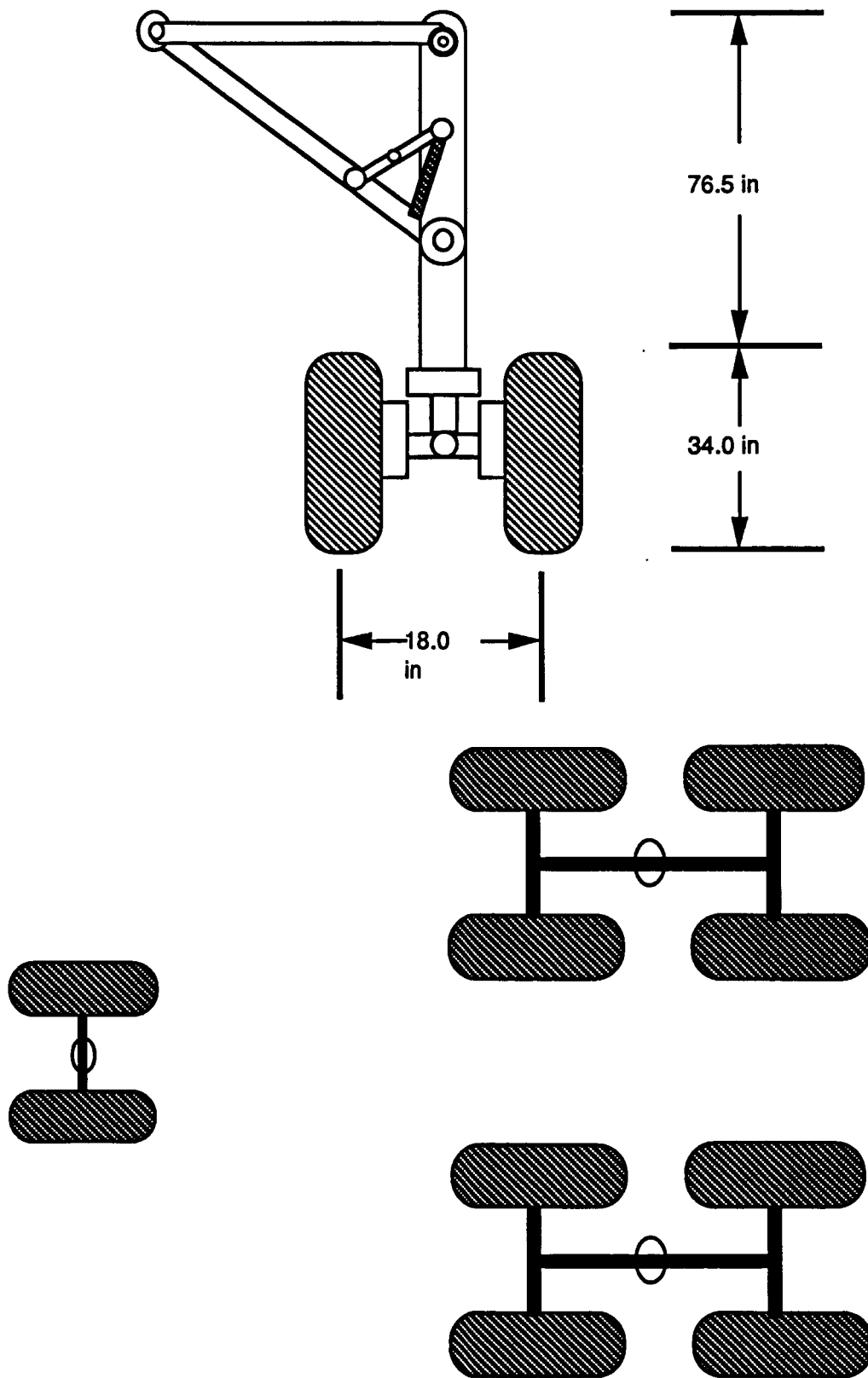
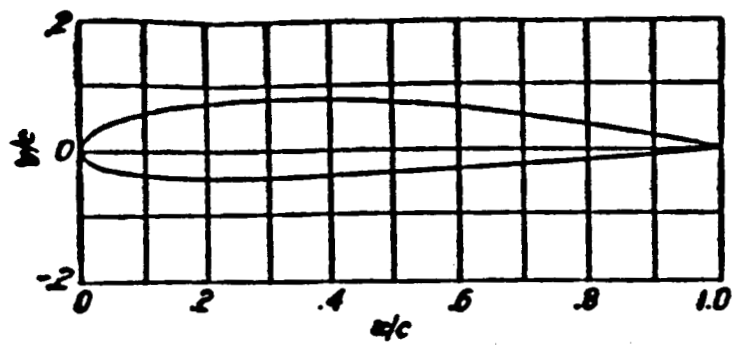
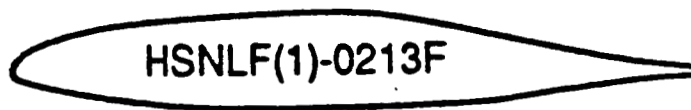


Figure 6: Dual Tandem Landing Gear Design



a) NACA 2412 Airfoil.



b) NLF-0213 Airfoil



c) NACA 0012-64

Figure 7. Airfoil Cross-Section of a) Main Wing, b) Canard, c) Tail.

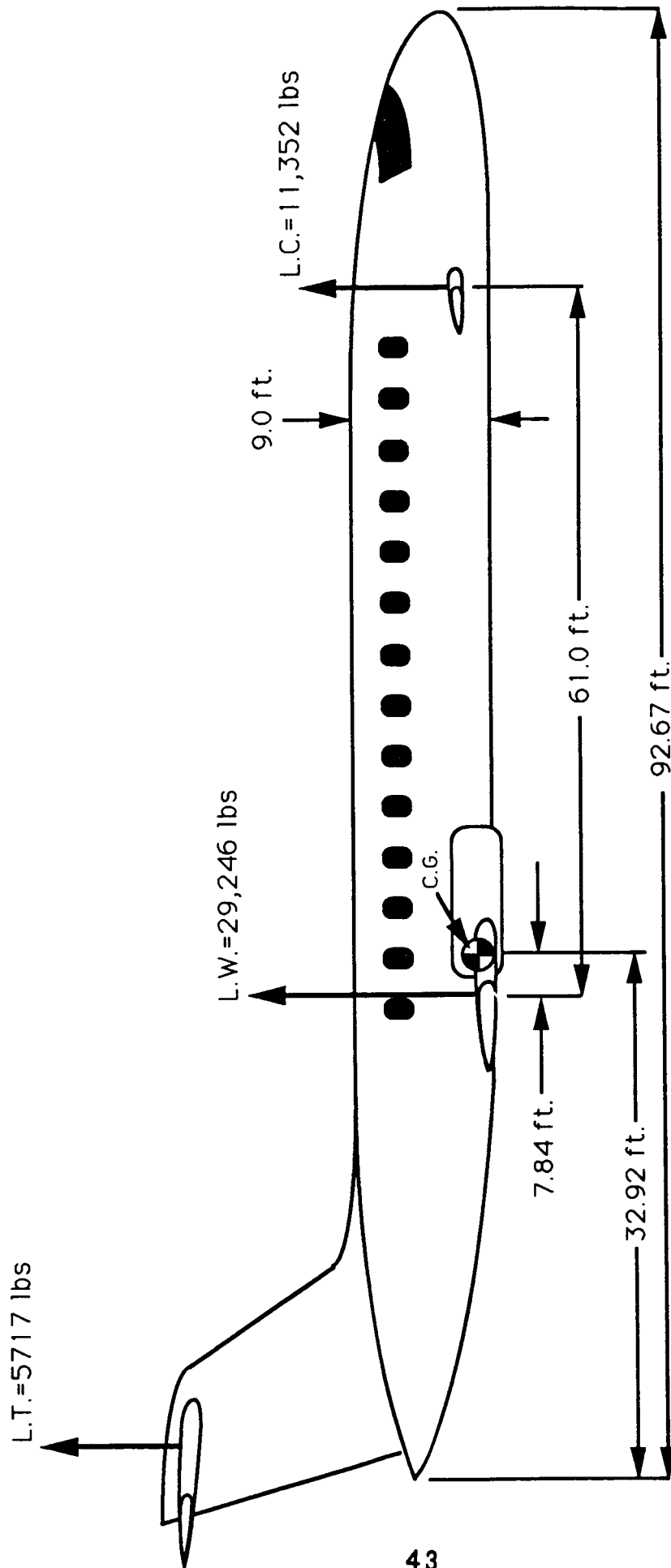


Figure 8: C.G. Locations and Lifting Force Locations

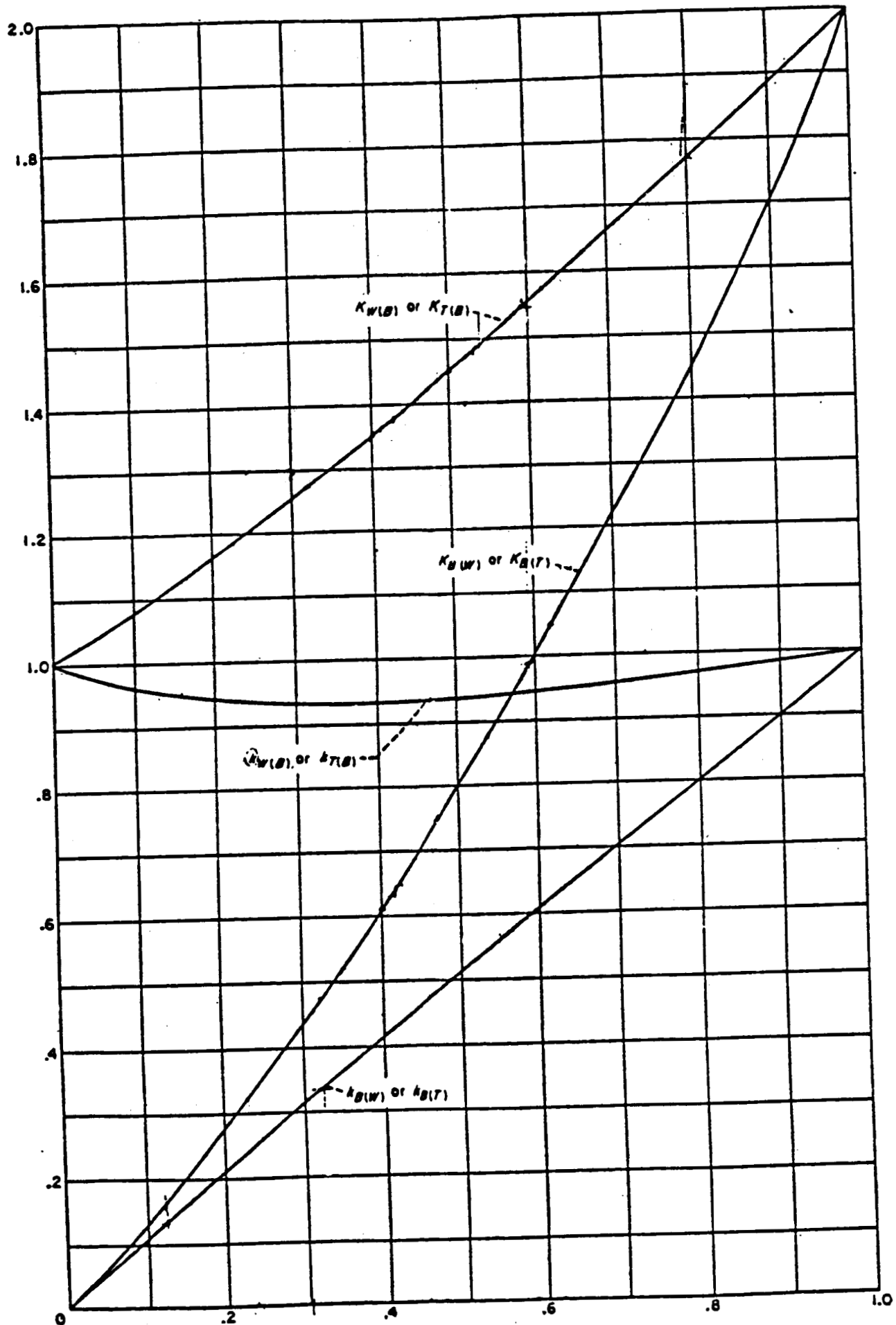


Figure 9. Body-on-Wing and Wing-on-body Interference Constants.

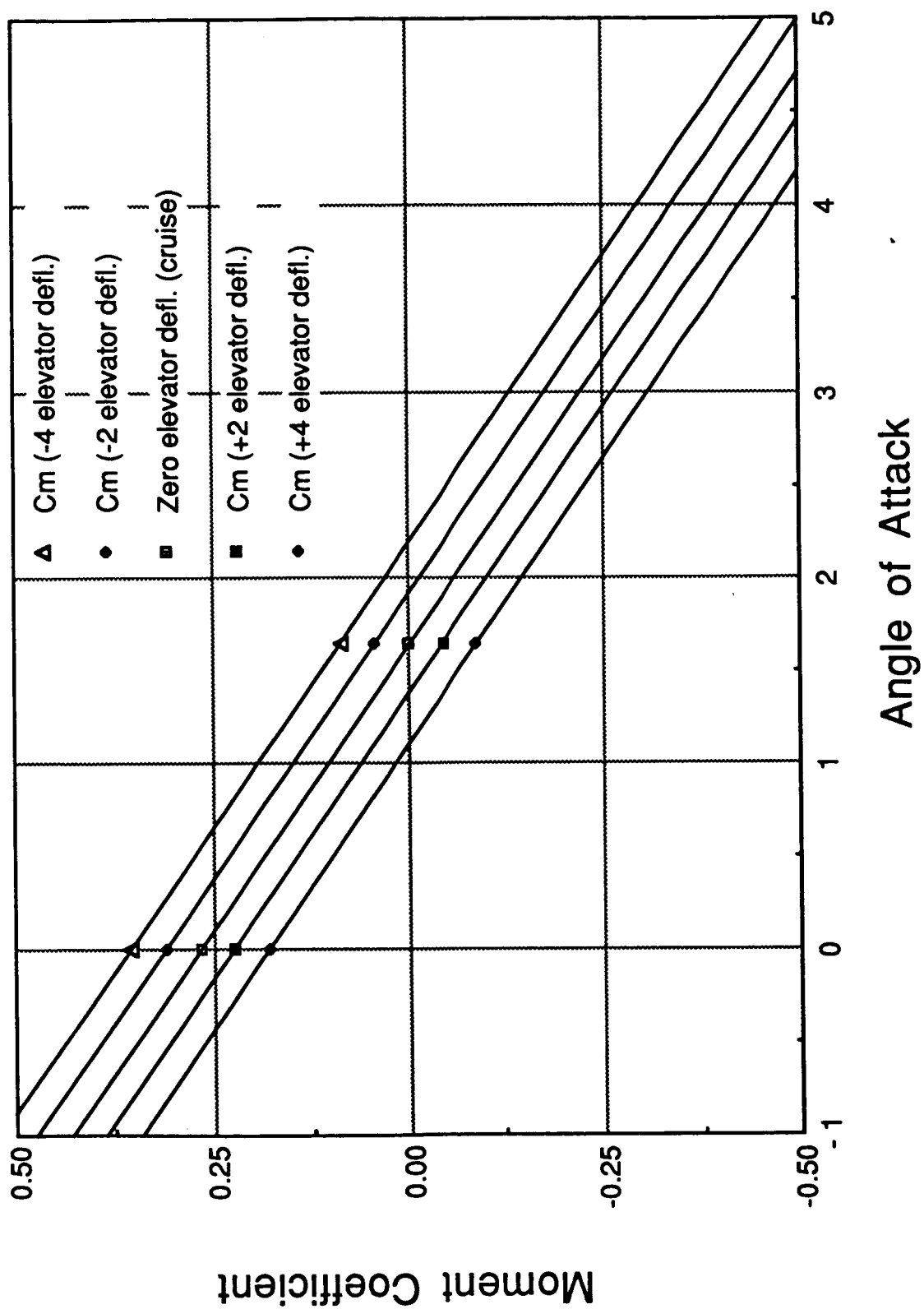


Figure 10: Plot of the Moment Coefficient vs Angle of Attack.

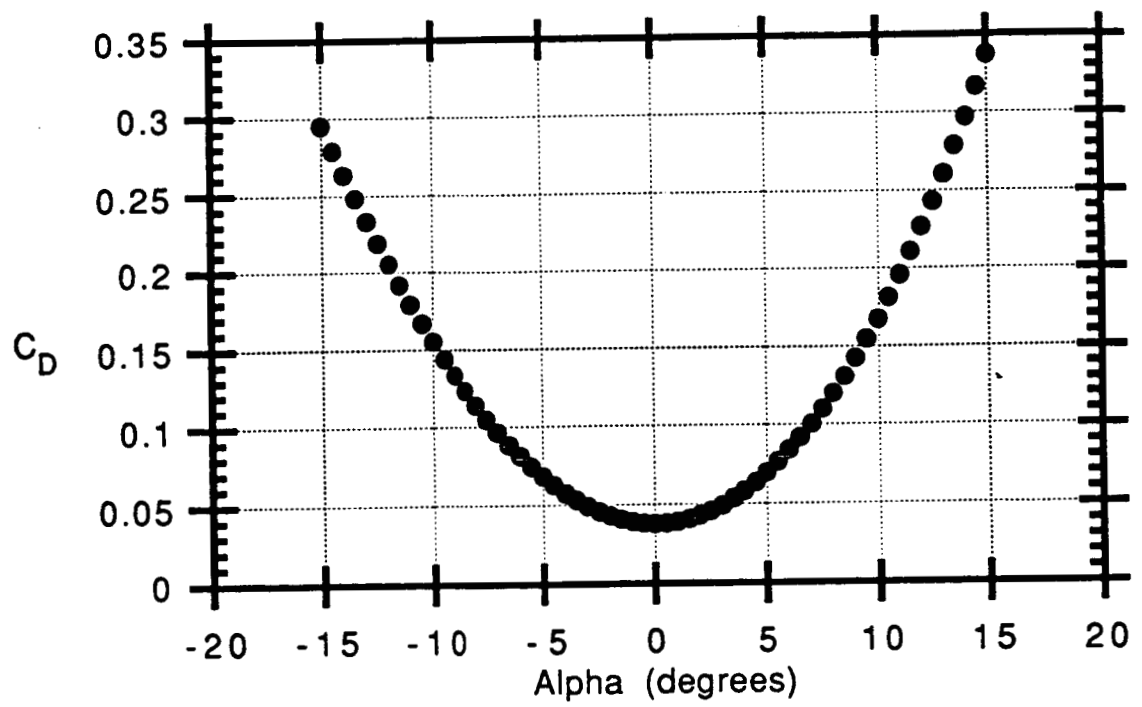


Figure 11a: C_D versus α at cruise.

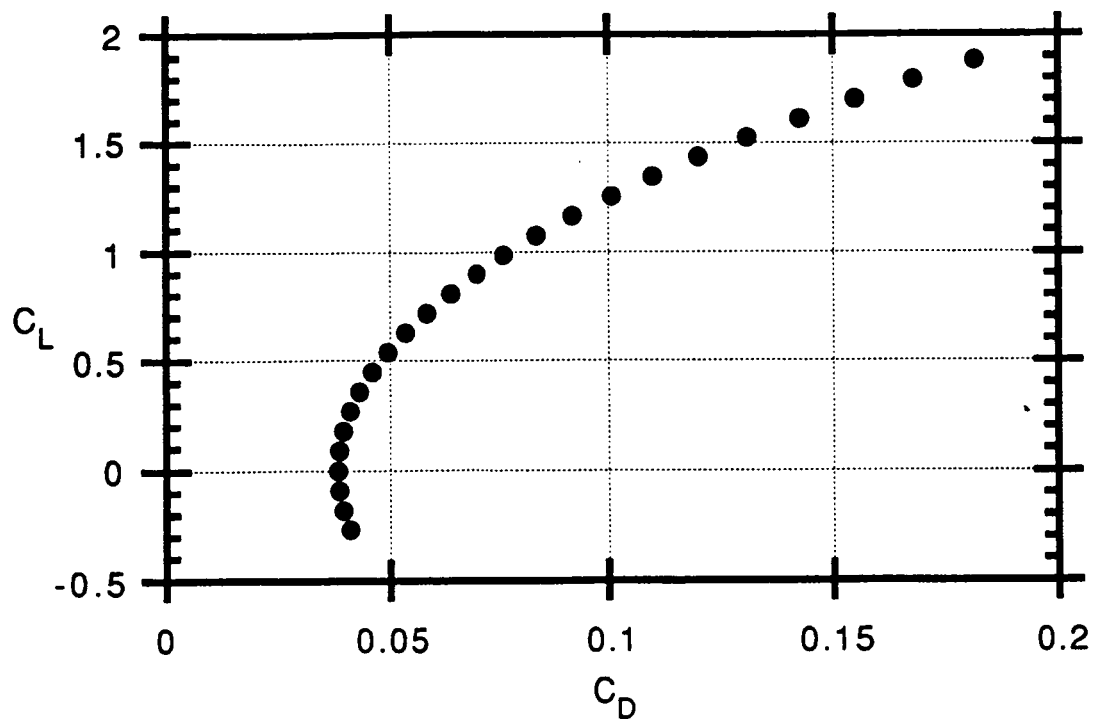


Figure 11b: Drag Polar at Cruise.

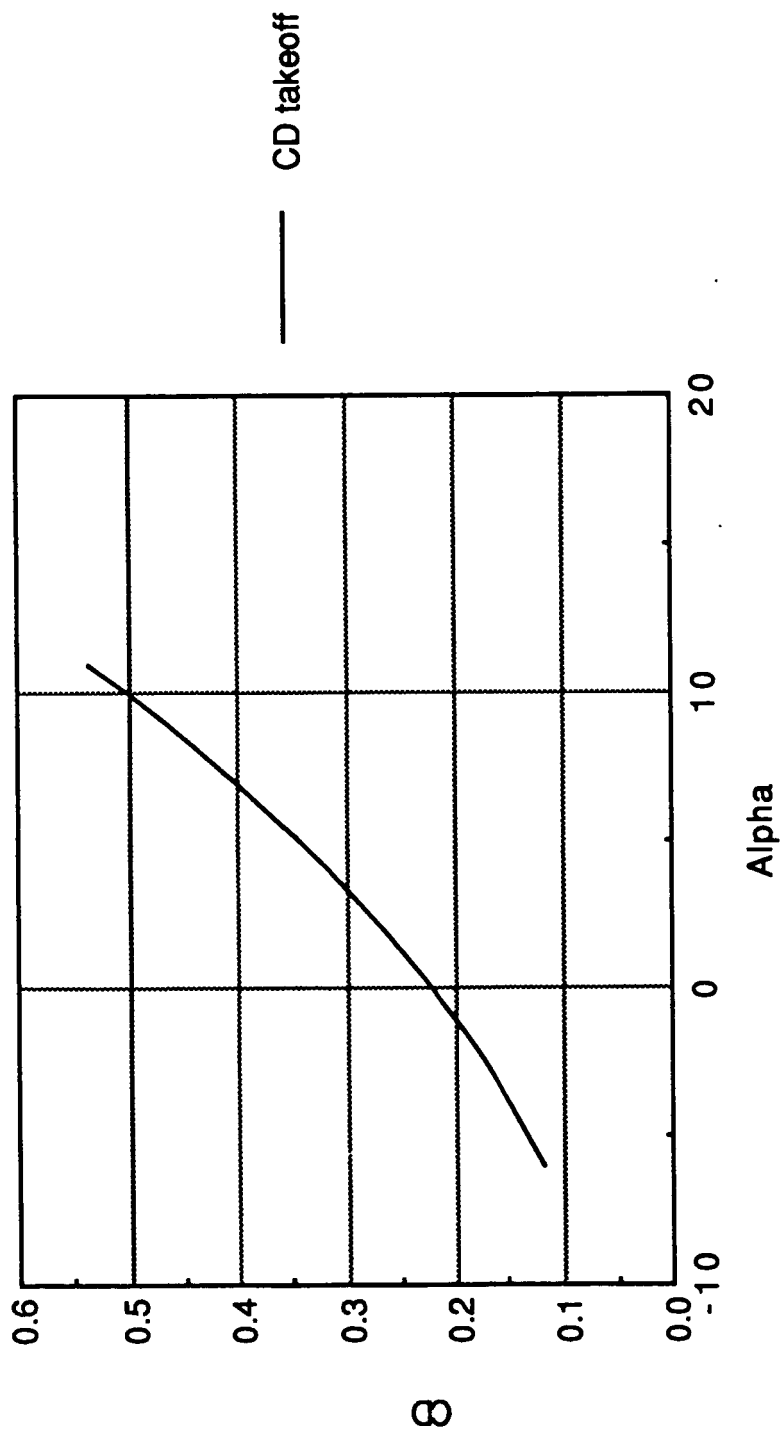


Figure 12a: CD versus CL during Takeoff (Flap=15)

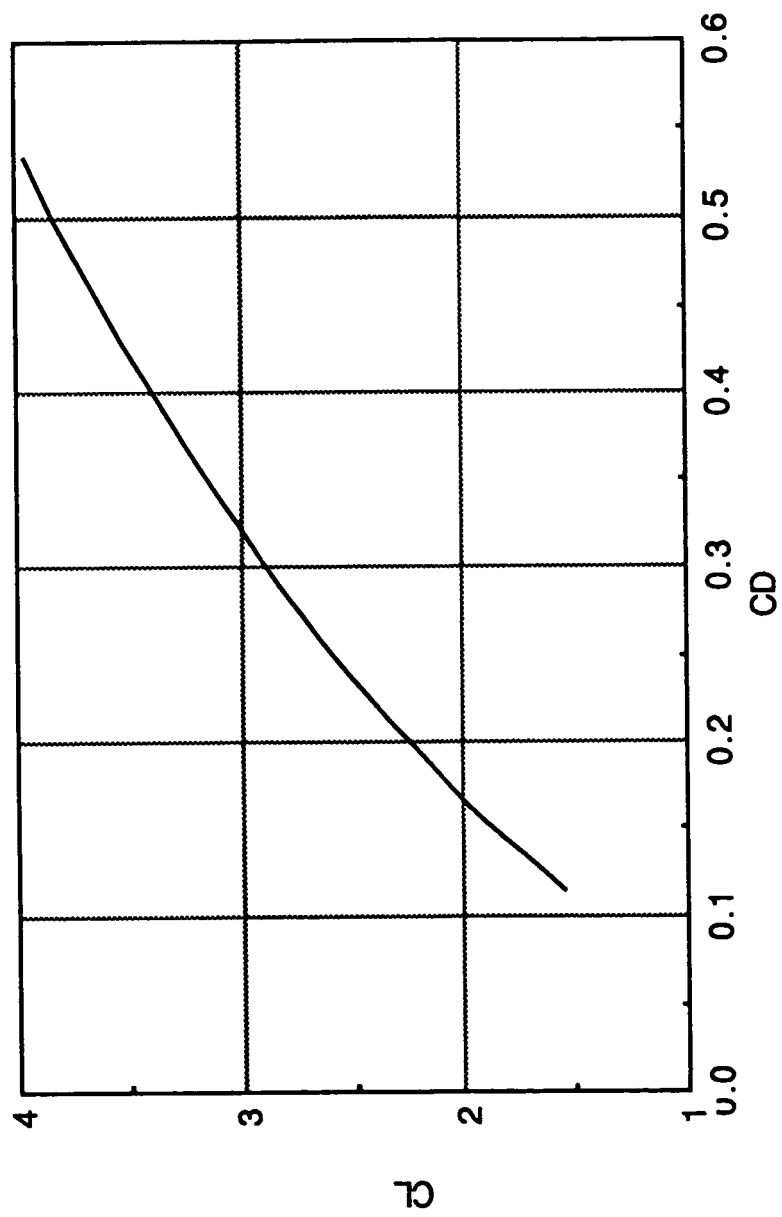


Figure 12b: Drag Polar for Takeoff (Flap=15)

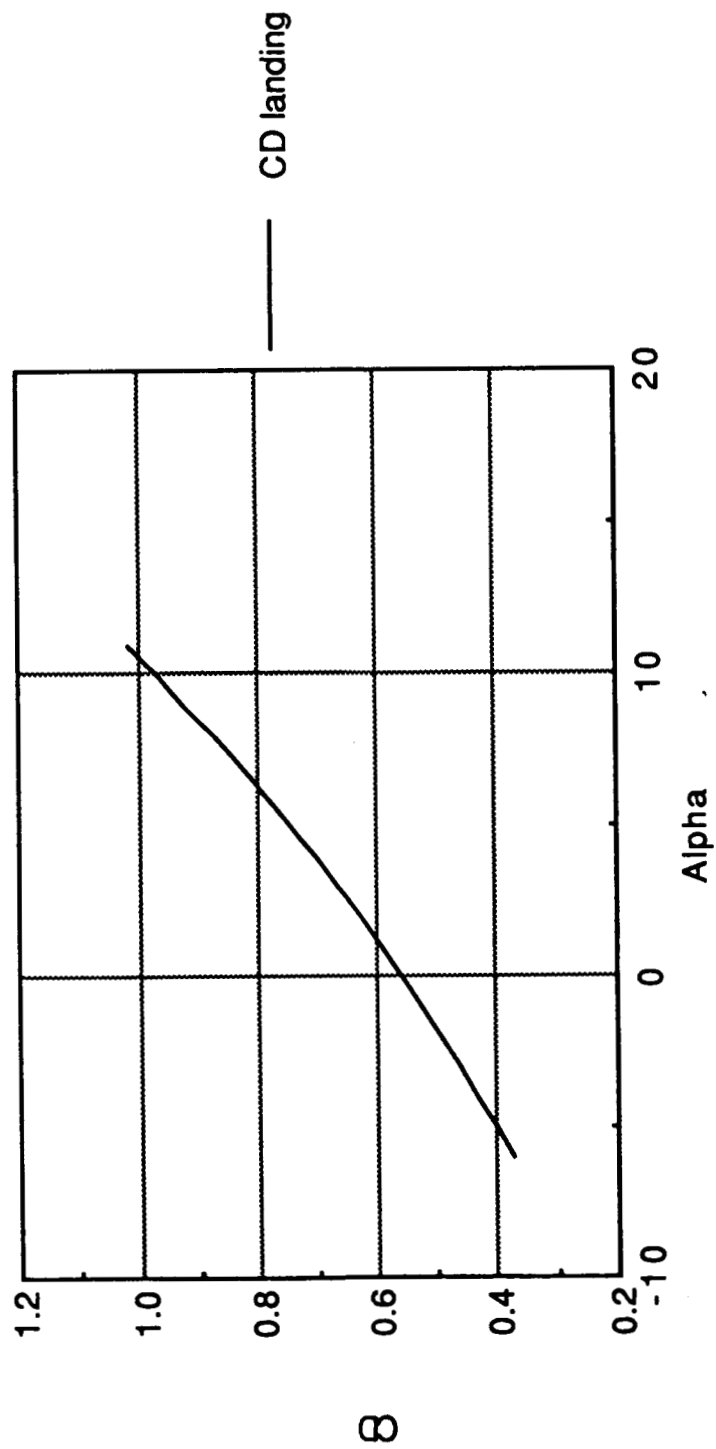


Figure 13a: CD versus Alpha during Landing (Flap=40)

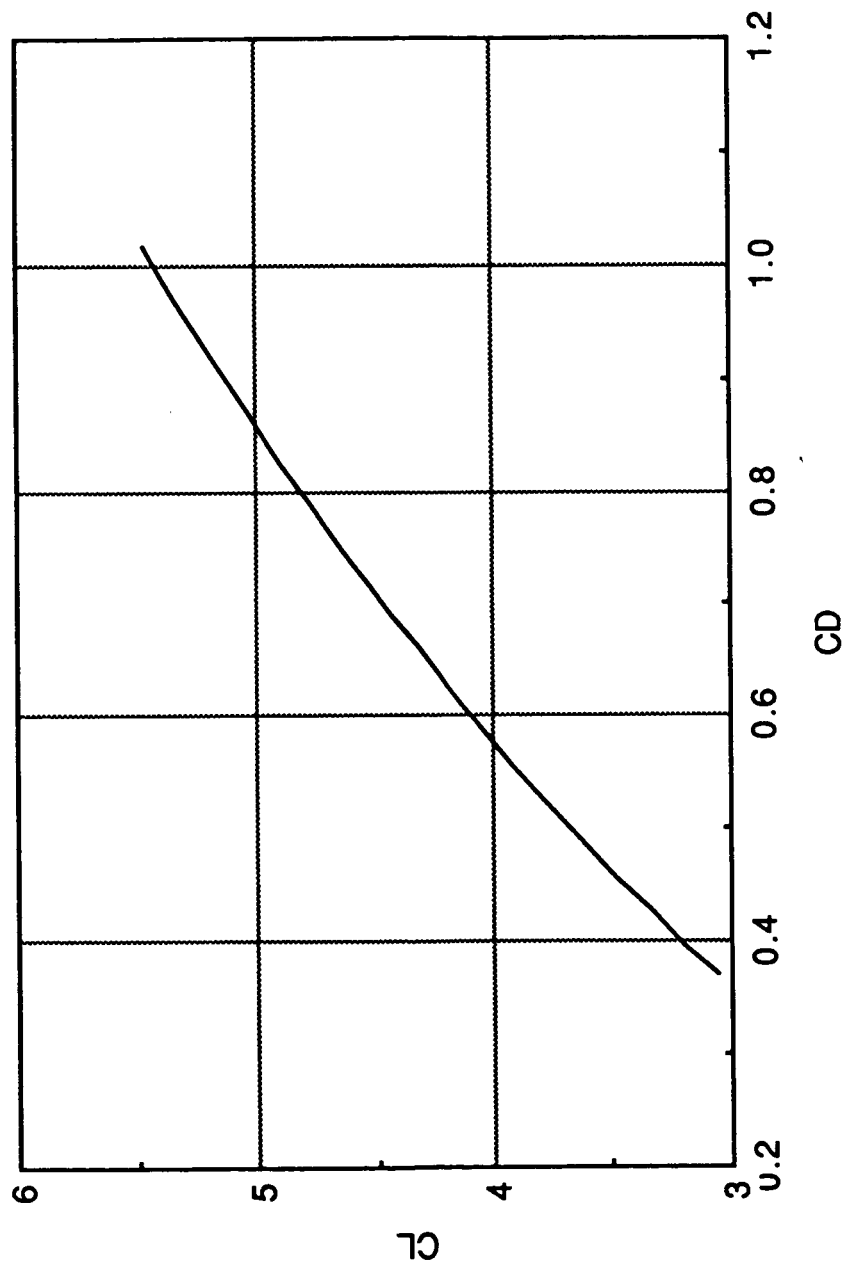


Figure 13b: Drag Polar for Landing (Flap=40)

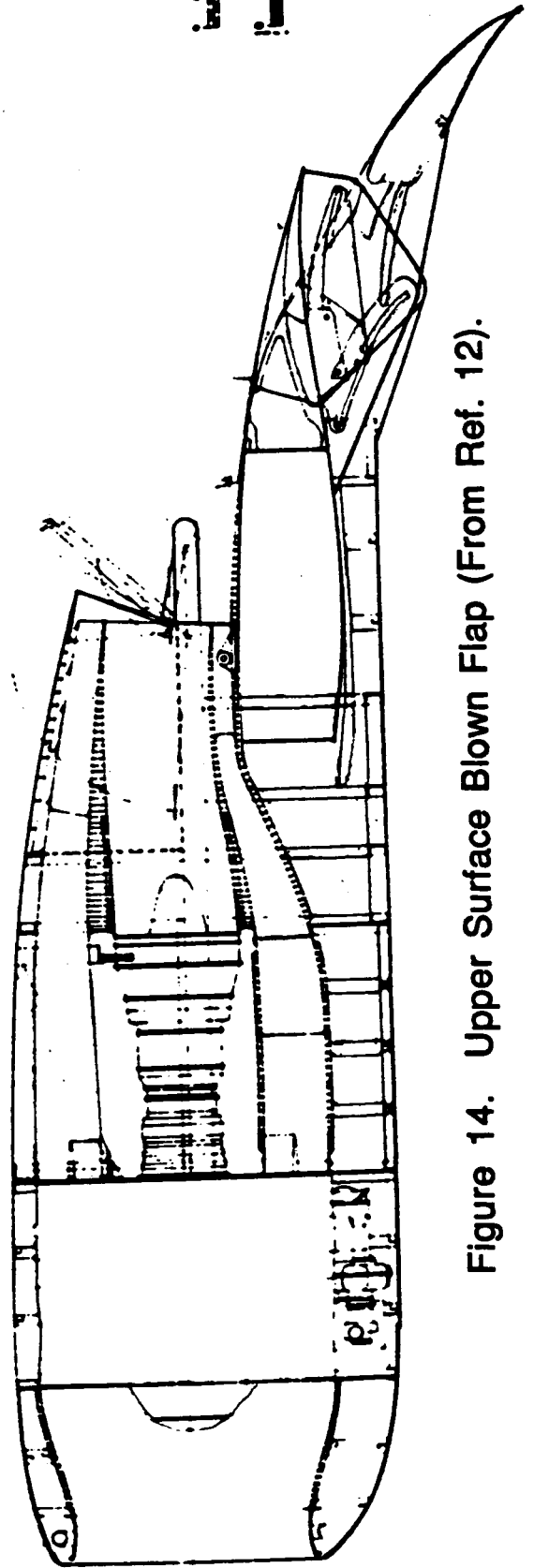
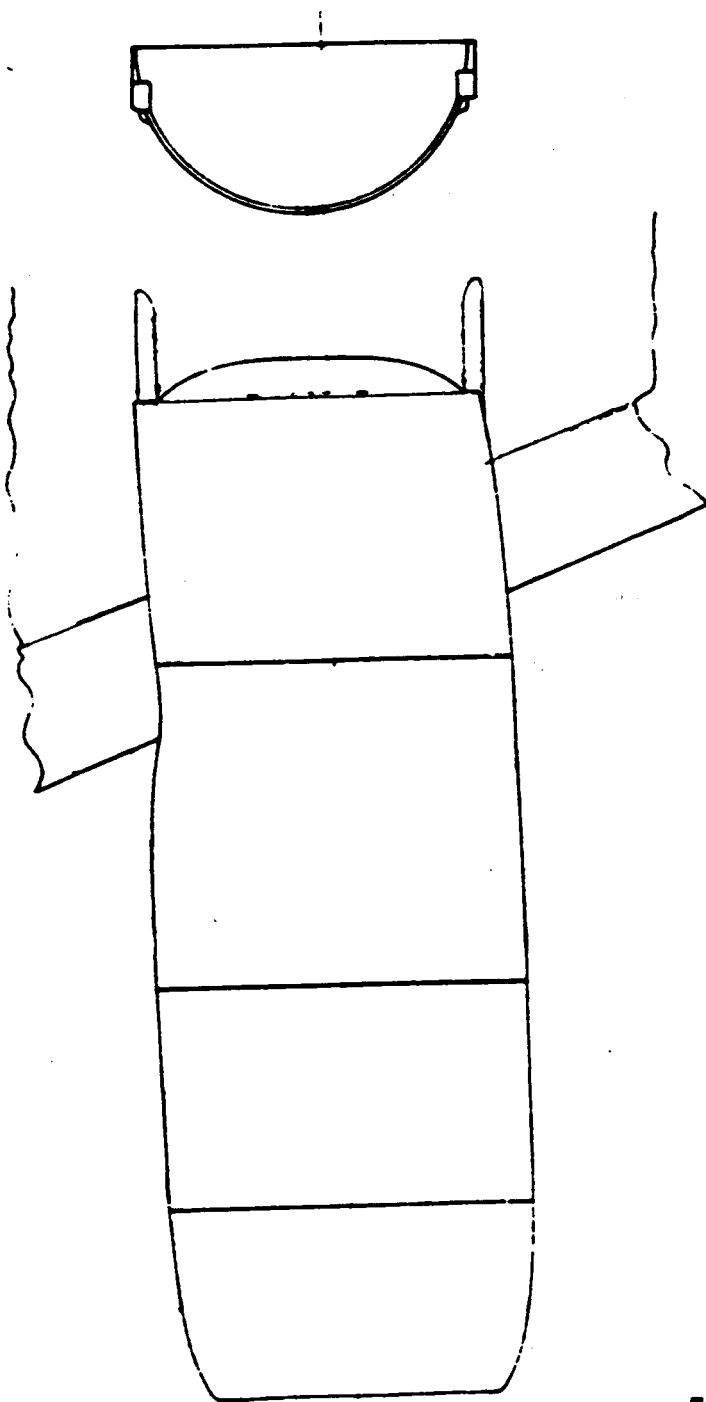


Figure 14. Upper Surface Blown Flap (From Ref. 12).

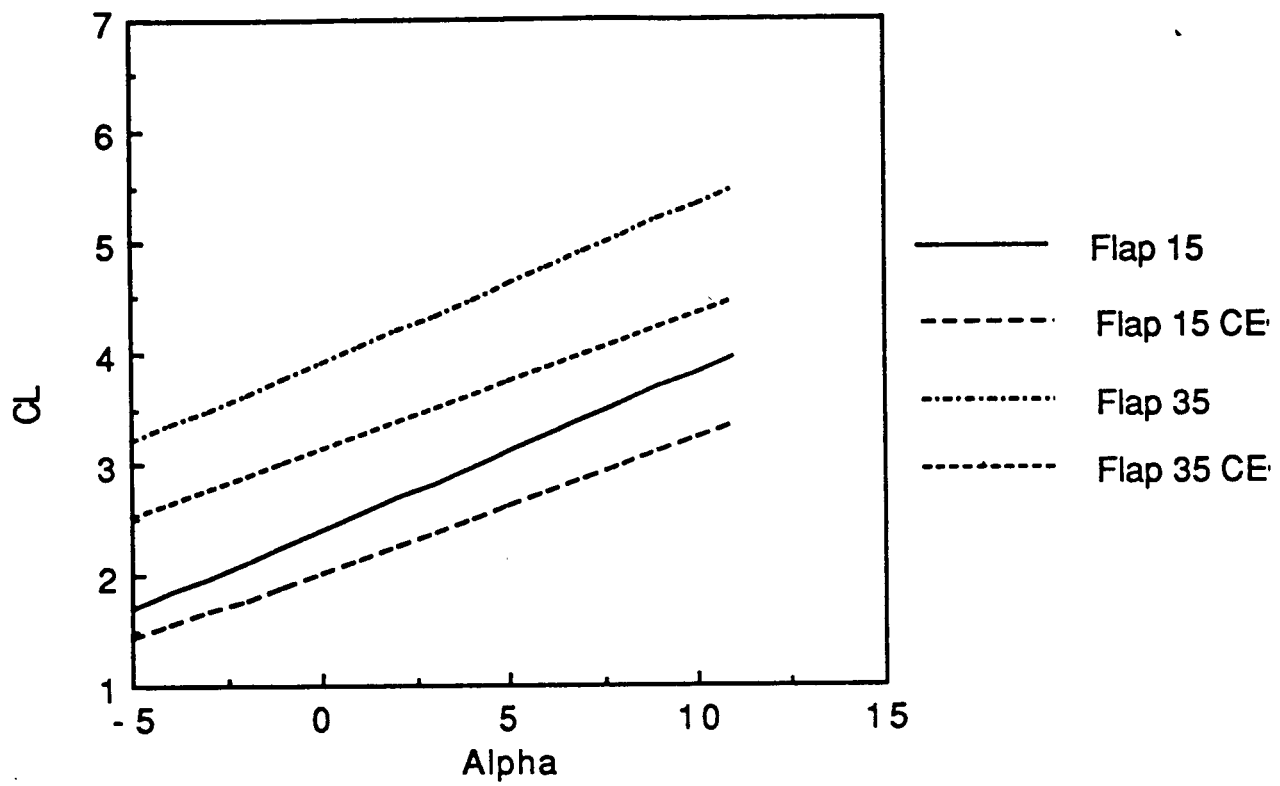


Figure 15: CL versus Alpha for Changes in Flap Deflection and CEO

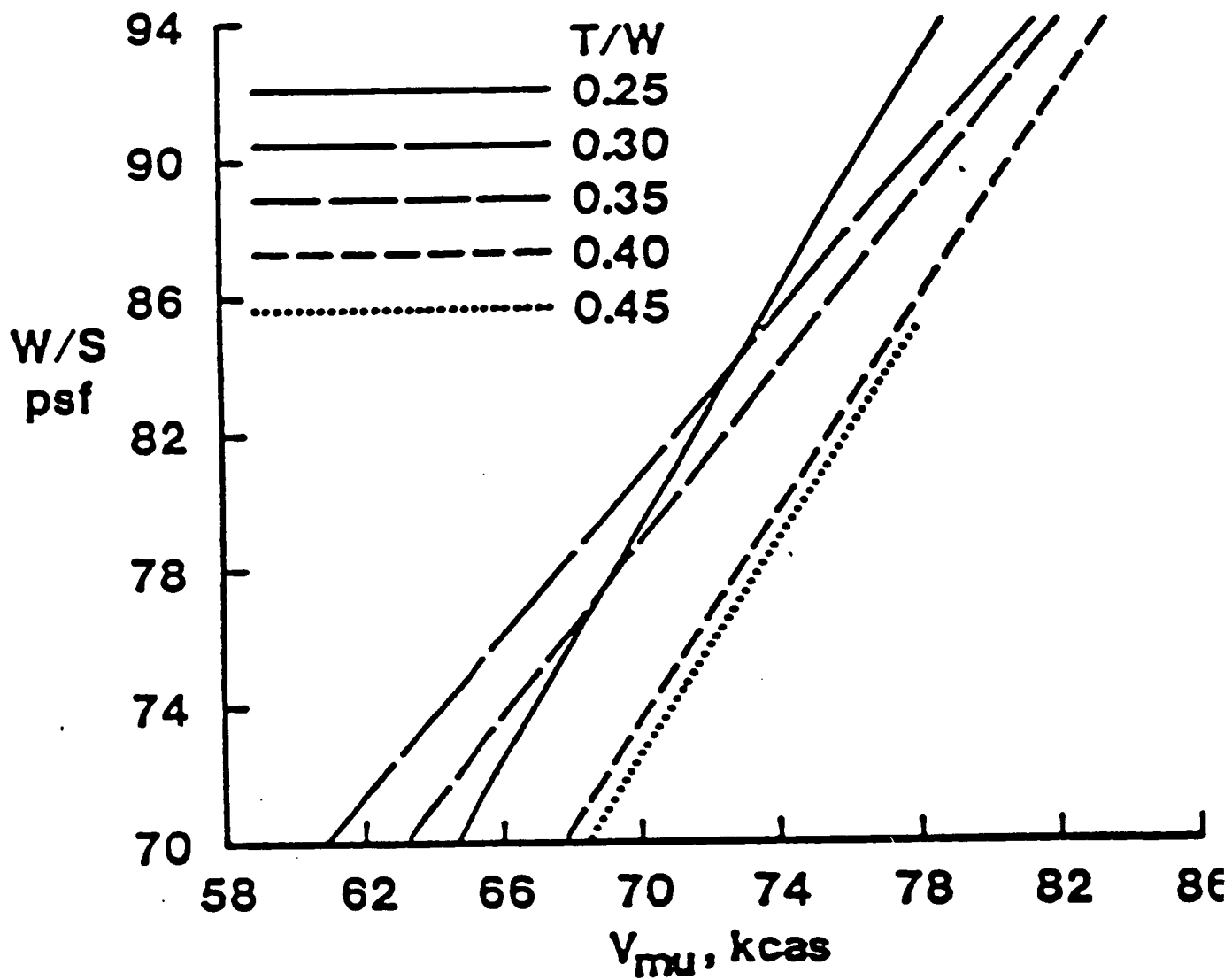


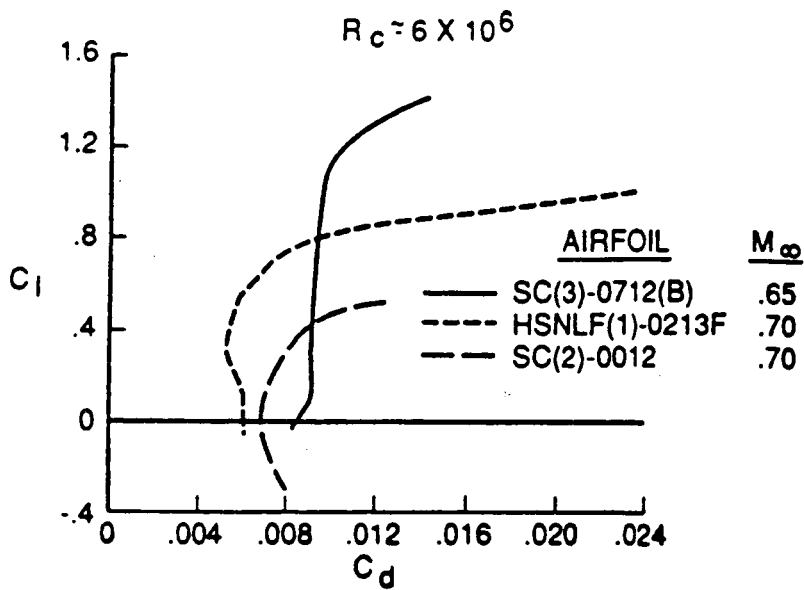
Figure 16. AEO minimum unstick airspeeds for five T/W values with DS flap=59 degrees, USB flap=0 degrees (From Ref. 12).

REFERNECES

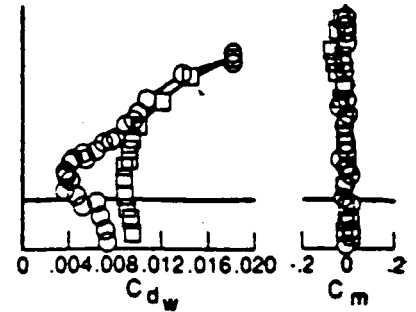
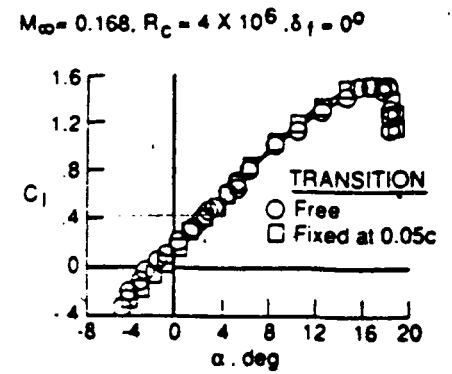
1. Torenbeek, Egbert, Synthesis of Subsonic Airplane Design, Delft University Press, Delft, The Netherlands, 1988.
2. McCormick Jr., Barnes W, Aerodynamics. Aeronautics. and Flight Mechanics, John Wiley & Sons, New York, 1979.
3. Budinski, Kenneth G., Engineering Materials: Properties and Selection (third edition), Prentice Hall, New Jersey, 1989.
4. ALCOA Aerospace Technical Fact Sheet: Alloy 2090-T83 Sheet Aluminum Company of America, Bettendorf, Iowa, 1990.
5. Reynold's Metals Co., Fact Sheet, Reynold's Metals Co., McCook, Illinois, 1991.
6. Aluminum Developments Digest, The Aluminum Association, Washington D.C., Fall 1990.
7. Shevell, R.S., Fundamentals of Flight. 2nd. ed., Englewood Cliffs, N.J., Prentice Hall, 1989.
8. Johnson, J. L. Jr., AIAA-83-2531 Exploratory Low-Speed Wind Tunnel Investigation of Advanced Commuter Configuration Including an Over the Wing Propeller Design, 1983.
9. Etkin, Bernard, Dynamics of Flight Stability and Control second. ed., John Wiley & Sons Inc., New York, 1982.
10. Roskam, Jan, Methods for Estimation Drag Polars of Subsonic Airplanes, University of Kansas, Lawrence, Kansas, 1973.
11. Spence, D.A., Some Simple Results for Two-Dimensional Jet-Flapped Aerofoils, Aeronaut. Quart., Vol. IX, Pt. IV, 395-406, November 1958.
12. Riddle, D.W., Innis R.C., Martin, J.L., AIAA-81-2409 Powered-Lift Takeoff Performance Characteristics Determined from Flight Test of the Quiet Short-Haul Research Aircraft (QSRA), November 1981.

13. Riddle, D.W., Stevens V.C., AIAA-86-2674 Performance Studies on the Application of Four-Engine and Two-Engine USB Propulsive Lift to the E-2C Aircraft; October 1986
14. Honeywell Inc., 535 West Bell Road, Glendale, Arizona 85308, Printed September 1989.
15. Bendix/King, Allied Signal Aerospace Company, 400 North Rogers Road, Olathe Kansas 66062-1212, Printed January 1990.

APPENDIX A

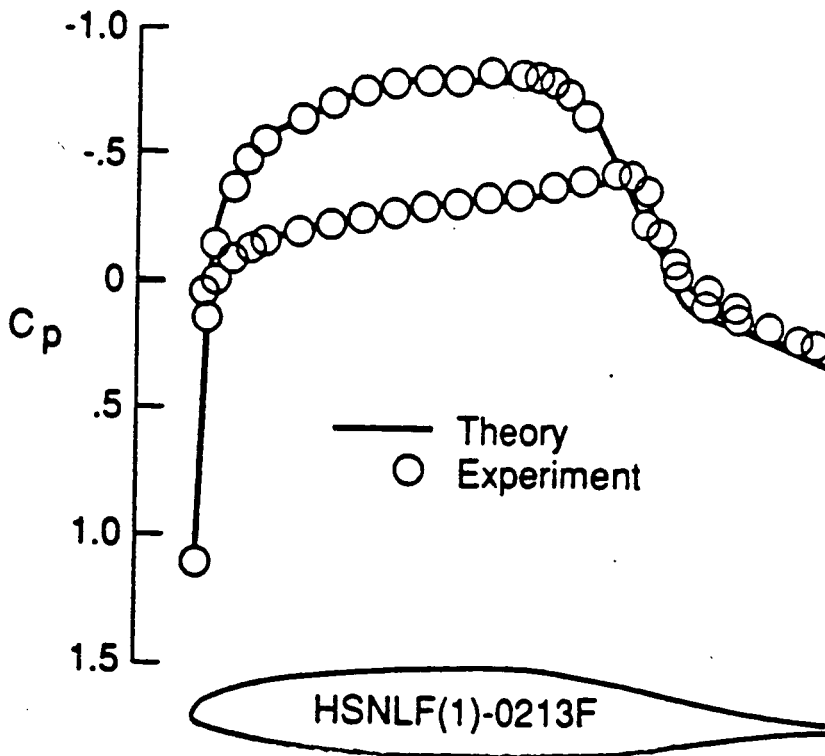


Comparison of experimental drag polars for medium-speed laminar and turbulent airfoils.

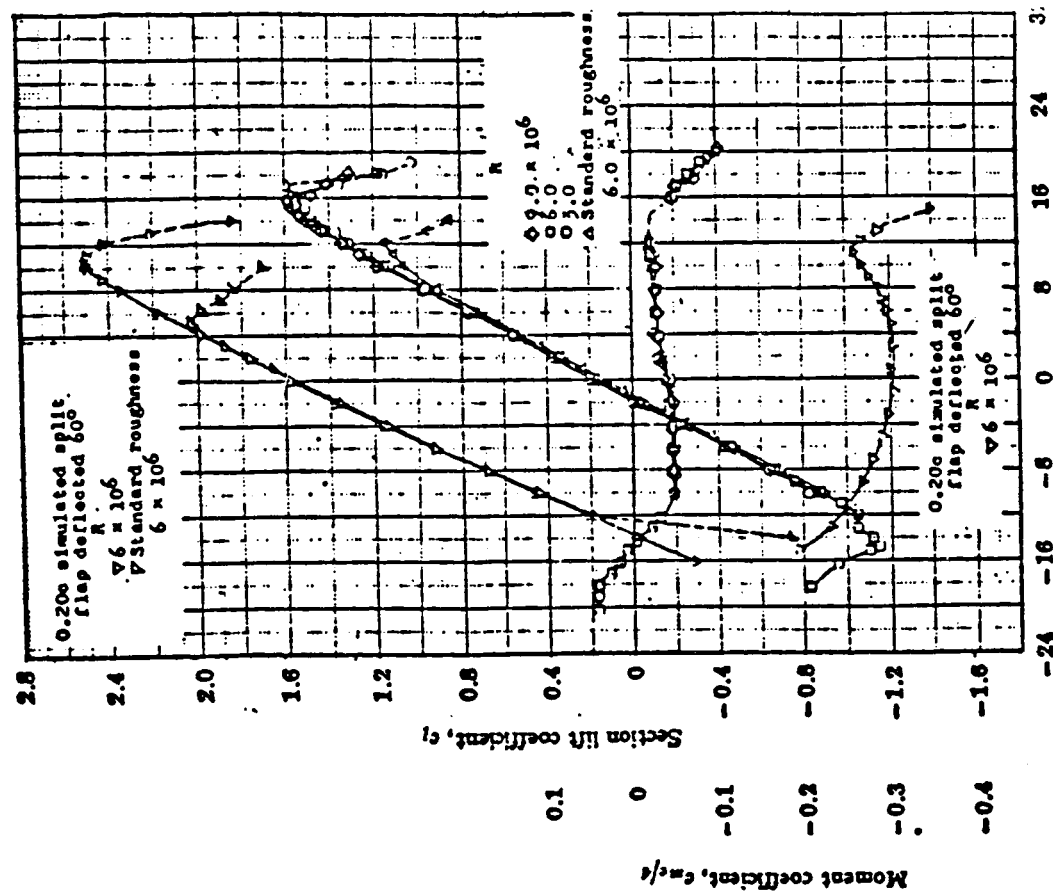


Measured section characteristics for the HSNLF(1)-0213 airfoil with fixed and free transition.

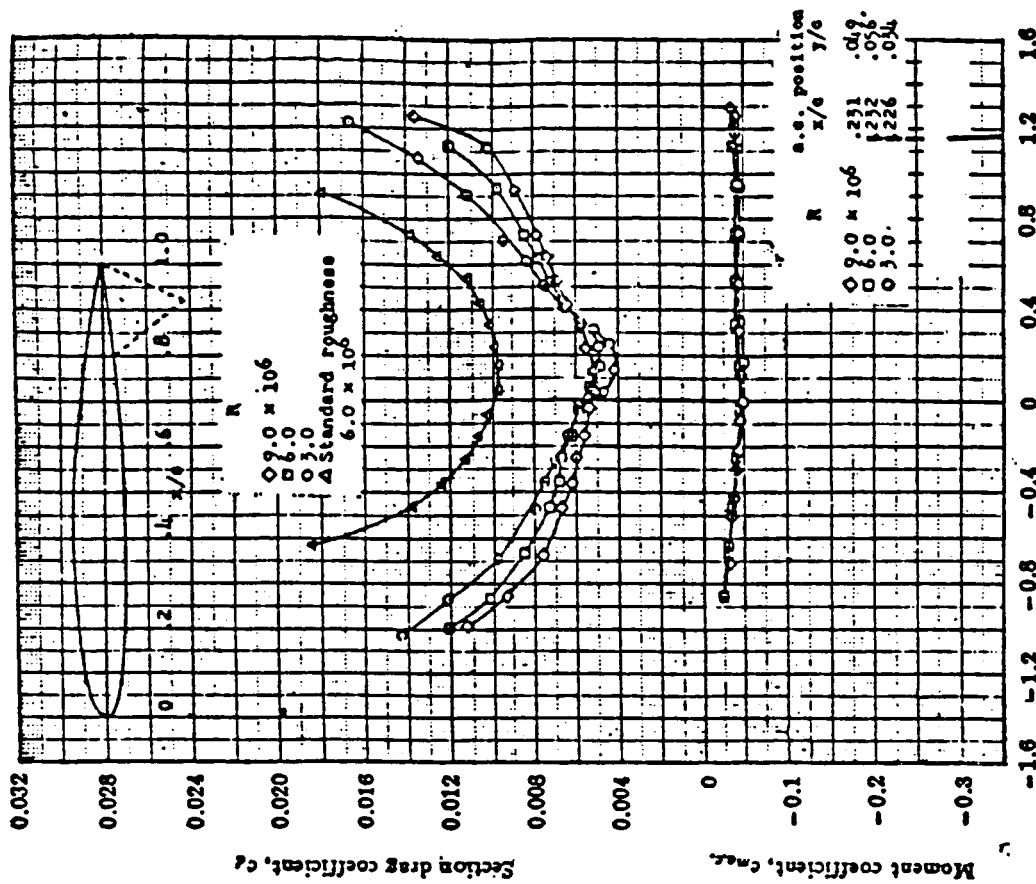
$M_\infty = 0.7, C_L = 0.26, \alpha = -3.4^\circ, R_c = 4.3 \times 10^6$



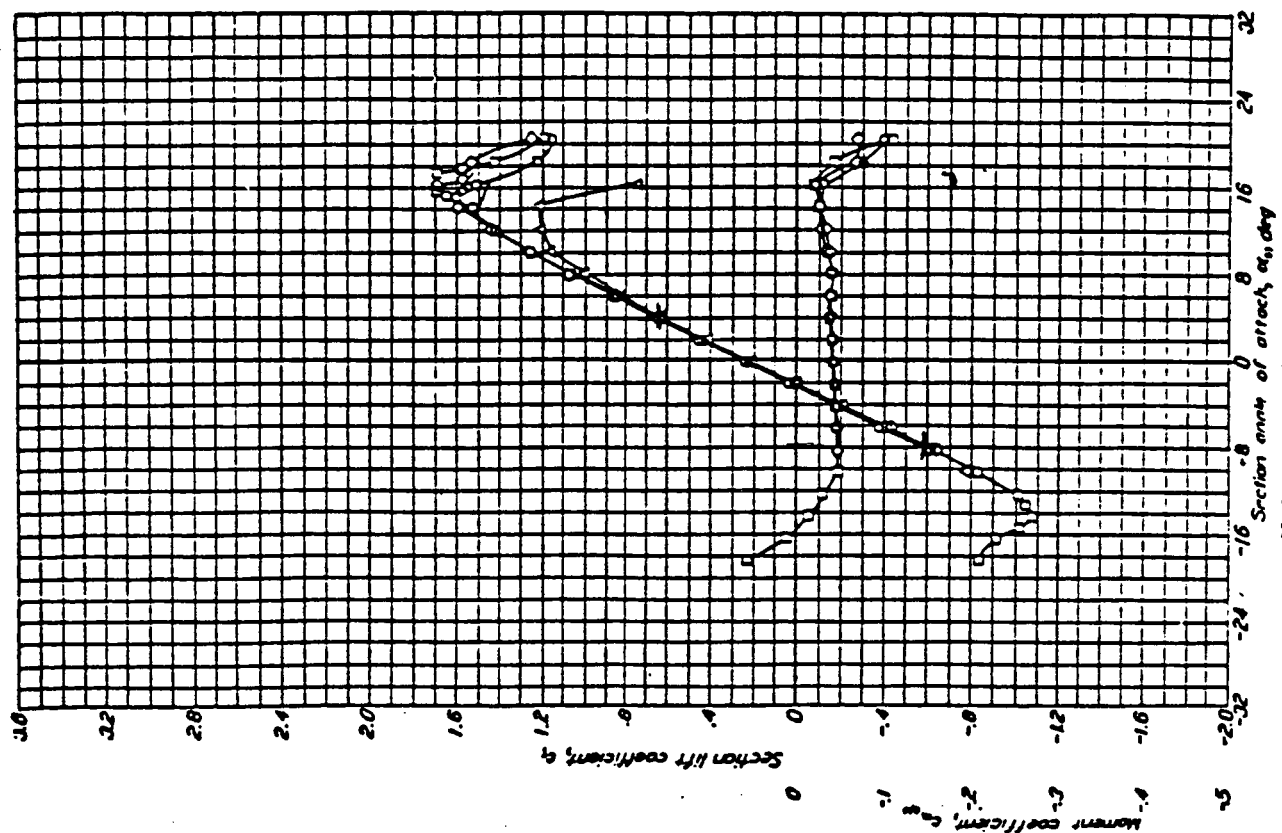
Comparison of experimental and theoretical pressure distributions on the HSNLF(1)-0213 airfoil.



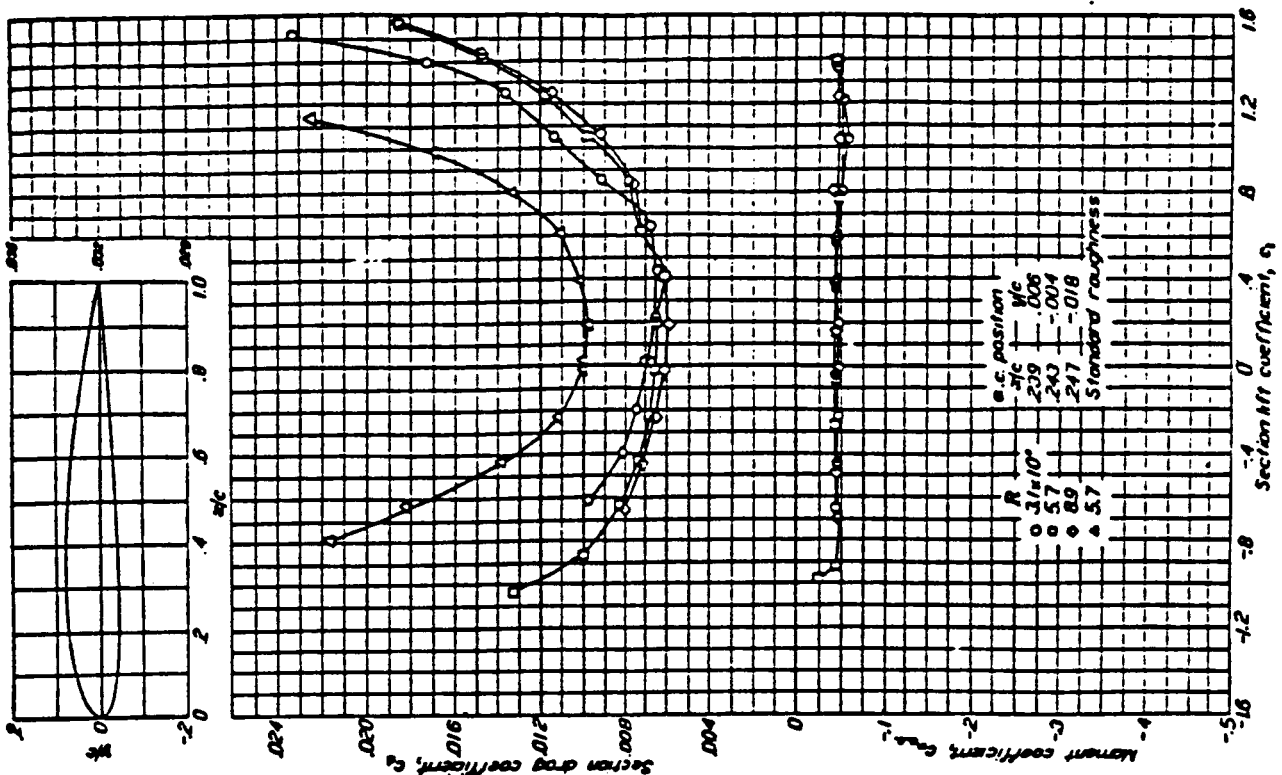
Section lift coefficient, c_l
 NACA 0012-04 Wing Section,
 $\alpha = 0.8$ (modified), $c_{l_0} = 0.2$ (Continued)



Section lift coefficient, c_l
 NACA 0012-04 Wing Section,
 $\alpha = 0.8$ (modified), $c_{l_0} = 0.2$



NACA 2412 Wing Section



NACA 2412 Wing Section (Continued)

a.c. position	
x/c	y/c
0.31	0.08
0.57	0.04
0.89	0.018
1.0	0.018
Standard roughness	